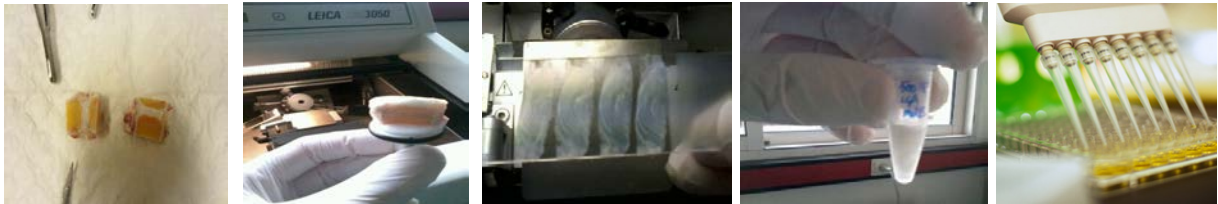


**Utrecht University,  
Faculty of Veterinary Medicine  
Research project Master GD**

# **The role of Prostaglandin E2 in intervertebral disc degeneration in dogs**

Utrecht, 2014

Maarten H. de Bie, BSc




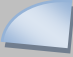
*Supervisor: drs. N. Willems, PhDc*



# Table of contents

---

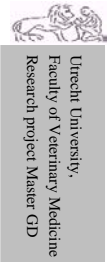
	 <i>Page number</i>
<b>Abstract</b>	<b>2</b>
<b>Introduction</b>	<b>2</b>
<b>The intervertebral disc</b>	<b>2</b>
<b>Intervertebral disc degeneration</b>	
<b>Appearance, etiology and incidence</b>	<b>3</b>
<b>Diagnosis</b>	<b>5</b>
<b>Therapy and Prognosis</b>	<b>6</b>
<b>Prostaglandin E2</b>	
<b>Origin and background</b>	<b>8</b>
<b>Prostaglandin E2 and intervertebral disc degeneration</b>	<b>8</b>
<b>Aim of the Study</b>	<b>9</b>
<b>Material and Methods</b>	<b>10</b>
<b>Results</b>	<b>12</b>
<b>Discussion</b>	<b>13</b>
<b>Conclusion</b>	<b>17</b>
<b>Acknowledgements</b>	<b>17</b>
<b>References</b>	<b>17</b>
<b>Appendices</b>	
<b>Appendix A: list of result tables</b>	<b>20</b>
<b>Appendix B: list of result figures</b>	<b>25</b>



Supervisor: drs. N. Willems, *PhDc*

# The role of Prostaglandin E2 in intervertebral disc degeneration in dogs

Utrecht, 2014

Maarten H. de Bie, *BSc*

## Abstract

**Introduction:** Intervertebral disc (IVD) degeneration is a common problem in dogs and humans, and has significant effects on spinal biomechanics. Present-day therapies are either conservative or surgical and do not solve the problem of the degenerative process. In the search for targeted therapies and more clarification towards the process, prostaglandin E2 (PGE2) is proposed to have impact on the disc matrix. Multiple in vitro studies have revealed increased levels PGE2 in degenerative discs, but thus far in vivo studies are lacking. The beagle dog breed has been shown to be a valuable translational model to study spontaneous IVD degeneration in humans.

**Methods:** In an on-going study from N.Willems (*PhDc*) two types of hydrogels and microspheres were loaded with a COX-2 selective inhibitor (Celecoxib, CXB) and injected intradisally in Beagles to accomplish a slow release of and subsequently a reduction in PGE2 in the IVD. To determine the PGE2 contents, three types of ELISAs of two different manufacturers (R&D and ENZO) were tested. As part of the overarching study, this research project was designed to establish the most reliable ELISA. In order to preserve valuable canine test material bovine material was included. IVDs from two cowtails were collected from the slaughterhouse. From the IVDs transversal and sagittal cuts and subsequently cryoslides were performed and the resulting sample material was gathered in Ambion<sup>®</sup> lysis buffer. Nucleus pulposus (NP) material was separately collected, and after Ambion<sup>®</sup> lysis, the resulting NP supernatant was applied in the available ELISAs. Dilution outcomes, standard deviations (SD), covariance rates (CV), spike-and-recovery experiments and intra-assay precisions (IAPs) were compared, and PGE2 levels were relativized to quantified protein concentrations by using the Thermo Scientific Pierce<sup>®</sup> BCA protein Assay. All results were calculated by Microplate Manager<sup>®</sup> (MPM) 6 Software.

**Results:** Particularly the IAP, spike, and dilution results demonstrated inconsistency in the R&D, with especially high SDs in the lower ranges. The outcomes of both ENZO ELISAs were more reliable, but PGE2 concentrations in the canine and bovine IVDs appeared to be less than expected. In the bovine ENZO-HS the PGE2 amounts of sample dilutions were immeasurably low, but in the canine material, compared to the ENZO, the ENZO-HS was steadier and better able to quantify the PGE2 levels in these lower ranges.

**Conclusion:** As a result, the ENZO-HS was considered to be the most appropriate test for the further research in the Beagle experiment.

**Keywords:** intervertebral disc degeneration; Prostaglandin E2 (PGE2); ELISA; dogs

## Introduction

Back disorders are frequently encountered in humans as well as in dogs<sup>1-5</sup>, and intervertebral disc (IVD) degeneration is considered to be one of the most common causes<sup>3,6-9</sup>. In dogs, diseases related to degeneration of these IVDs often result in severe neurological insufficiencies associated with unfavorable prognoses<sup>10,11</sup>. There is a high incidence of IVD-related problems in both humans and dogs<sup>3,5,12-14</sup> and specific dog breeds such as the Beagle serve as valuable spontaneous animal models for IVD degeneration in humans<sup>15</sup>. Present-day therapies focus on alleviating pain and symptoms via symptomatic and/or surgical intervention, but do not always provide sufficient results and do not solve the problem of the degenerative process. Therefore, there is a strong need for innovative therapies that intervene or reverse the processes of degeneration. To achieve this, more knowledge and understanding towards the etiopathology of IVD degeneration is required. The possible role of Prostaglandin E2 (PGE2) shall be outlined, and in this research project the most reliable ELISA to quantify PGE2 in Beagle IVDs will be established. After initially outlining the general aspects of the intervertebral disc and IVD degeneration in dogs, these research results will be discussed.

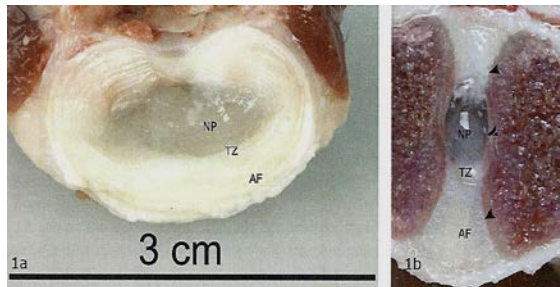
## The intervertebral disc

In general, the vertebral column of the dog is composed of a series of seven cervical, thirteen thoracic, seven lumbar and three sacral vertebrae, which are supplemented with a highly ranging number of coccygeal vertebrae that varies from six to twenty-three, depending on the dog's breed along with existing individual differences<sup>16-18</sup>. The vertebral bodies are joined together by numerous muscles, ligaments and articular processes, and fibrocartilaginous discs interconnect almost all adjacent vertebrae<sup>19</sup>. These so-called intervertebral discs (IVDs) are present between the second and third cervical vertebra (C2-3) and extend to the latest vertebra in the tail, thereby excluding the three sacral vertebrae (S1-3) which fuse at an early age to form the sacrum<sup>16,18</sup>. Thus, dogs have twenty-six IVDs, without taking the highly variable coccygeal region into account. Development, growth, ageing, mechanical stress and degenerative processes all influence disc composition<sup>20</sup> and together, all the IVDs contribute to up to twenty percent of total vertebral column length<sup>16</sup>.

The IVDs are essential structures of the spine, each of them composed of two major distinct zones: an outer, multilayer fibrocartilaginous ring,

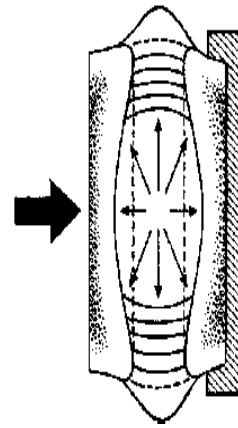


known as the annulus fibrosus (AF), which surrounds a more gelatinous, translucent core that is called the nucleus pulposus (NP)<sup>21,22</sup>. Both essentially different regions are shown in *figure 1* and have their own unique properties designed for specific functions, collectively creating a structure that is able to transmit a variety of biomechanical forces between vertebral bodies, in addition to provide indispensable flexibility and stability to the respective spinal segments<sup>23,24</sup>.



**Figure 1** – Transverse (a) and sagittal (b) section through a L5-L6 intervertebral disc of a mature non-chondrodystrophic dog, showing the nucleus pulposus (NP) and the annulus fibrosus (AF), (Modified description, from Bergknut et al<sup>23</sup>).

To fulfill these physiological and mechanical functions, the IVD is largely dependent on the quality of its extracellular matrix<sup>25</sup>. This is a three-dimensional network in the NP, mainly composed of collagen type II fibers and proteoglycans, whose are intimately connected by covalent bonds<sup>24</sup>. As in humans, the IVD matrix in dogs is a dynamic structure that is constantly subject to processes of synthesis and breakdown<sup>25</sup>. It is the balance between these processes of synthesis and breakdown that determines the quality, integrity and characteristics of the matrix, and is therefore essential for the mechanical functional properties of the disc itself<sup>25</sup>. Collagen fibers provide tensile strength and attach the tissue to the bone and proteoglycan molecules are basically responsible for maintaining tissue hydration<sup>25</sup>. The strongly negatively charged glycosaminoglycan side chains of the proteoglycan molecules create a high osmotic gradient inside the NP, and as a result, loads of water molecules are attracted into the matrix<sup>24</sup>. The water is able to generate a hydrostatic pressure within the NP, which radiate in all directions<sup>26,27</sup>. Through this, forces can be evenly distributed over the whole IVD instead of only to be exerted on their initial locations. As a result the whole NP is triggered to diminish impacts of loading and likewise the AF is also turned on in order to help withstanding these biomechanical loads. This mechanism is greatly simplified illustrated in *figure 2*.



**Figure 2** - When a compressive load is passed through the normal intervertebral disc, a hydraulic pressure is generated within the gelatinous nucleus pulposus. This is radiated in all directions and is absorbed by the annulus fibrosus. The compressive force is, in this way, converted into a predominantly tensile force within the annular fibers which resists collapse of the intervertebral disc space. The tensile force is largest in the outer layers of the annulus fibrosus, and it is in this area that most injuries are sustained (redrawn, with modification, from White and Panjabi<sup>27</sup>).

The AF is a multilayer structure of concentric rings of fibrous lamellae that surrounds the NP. Collagen fibrils together with elastic fibers and proteoglycans are responsible for the most important biomechanical functions of the AF<sup>24,28</sup>. Collagen represents a major part of the annular tissue. With collagen type I as the predominating collagen type the annular layers mainly provide resistance to tensile forces<sup>29,30,31,32</sup>, whereas the NP with its collagen type II fibers is better in managing compressive forces<sup>33,34,35</sup>. Together with the aqueous NP that exerts internal hydraulic swelling pressure and the assistance of the other stabilizing elements of the vertebral column, such as the articular facets and ligaments, the AF forms a structure – the IVD – that functions as a “hydroelastic cushion”<sup>36</sup>, which is able to maintain its width when exposed to a variety of biomechanical loadings. The conformation, characteristics, different tasks and the cooperation of all these structures give the IVD the possibility to provide spinal stability and flexibility to lots of different loading conditions from various directions. In carnivorous animals, such as the dog, the IVD is hence a major component of a flexible vertebral column, necessary for high-speed running and hunting<sup>37,38</sup>.

## Intervertebral disc degeneration

### Appearance, etiology and incidence

There are many possible underlying causes that can adversely affect the normal functioning of the IVD. The majority of these are associated with the emergence of several biochemical changes within the NP and AF which eventually initiate a progressive structural and functional deterioration of the IVD, also known as IVD degeneration<sup>26,34,36,39,40-43</sup>. These changes do not only hinder functioning of the disc itself, they can secondarily influence by exposing other spinal structures, such as the spinal cord, ligaments<sup>44</sup>, vertebral bodies<sup>45</sup>, articular facets<sup>46-48</sup> and



surrounding musculature<sup>30</sup>, to compression or unusual loads<sup>49,50</sup>. IVD degeneration is not equal to IVD disease. Excluding for example traumatic hernias, in general applies that dogs with IVD-related diseases show signs of degeneration; however, IVD degeneration is not necessarily associated with clinical signs of disease, and therefore degenerated discs can also be encountered in practice as incidental findings<sup>13,39,51,52</sup>.

The process of IVD degeneration is an interplay of diverse etiological factors, such as repeated physical-mechanical overload, lifestyle and environmental factors, disturbances in the nutrient supply, cell senescence and death, altered levels of enzyme activity, and molecular changes within the matrix components<sup>25,43,53</sup>. In particular, IVD degeneration is regarded as a common age-related process that may gradually occur over the course of a lifetime, whereby especially wear and tear of the disc as well as intradiscal molecular changes seem to play an important role. The incidence of IVD degenerative disorders is increasing<sup>5,12-14,54-56</sup>. In a recent study published by Bergknut et al. (2011)<sup>12</sup> 3,5% of a population of 60.000 dogs was affected by an IVD degenerative disease before the age of 12 years. Besides, IVD related disorders are evidently overrepresented in certain dog breeds<sup>12</sup>, which strongly suggests a genetic predisposition among specific dog breeds<sup>25,43,53</sup>. Dachshunds are the most commonly affected dogs followed by Poodles, Pekingeses, Beagles, Lhasa Apsos, and Cocker Spaniels<sup>5,12-14,54-56</sup>. Bergknut et al. (2011)<sup>12</sup> described that 15-20% of all dachshunds were affected by IVD degenerative disorders within an age of 12 years. In humans, several genes associated with IVD degeneration have been identified<sup>25</sup>. These include genes of structural matrix molecules and genes responsible for signalling and metabolic pathways within or towards the disc. Smolders et al. (2011)<sup>57</sup> investigated Wnt/ $\beta$ -catenin signalling in healthy and early degenerative canine NPs by immunohistochemistry and gene expression, and found an upregulation of Wnt/ $\beta$ -catenin signalling activity in early stages of IVD degeneration. It is highly presumable that genetic influences are involved in canine IVD degeneration and thus further genetic research might be helpful to develop screening programs<sup>12,23</sup>. Apart from the suggested genetic predisposition, there also seems to be a difference in incidence between sexes<sup>12,54</sup>. Recent research results from Bergknut et al. (2010)<sup>12</sup>, shows a significantly greater risk in acquiring IVD-related disorders in male dogs than in female dogs. Although unproven in dogs, it is considered that the higher oestrogen level in female persons has beneficial and protective effects to the intervertebral discs<sup>54,58</sup>, by its unique ability to

regenerate bone-collagen after deterioration<sup>58</sup>. This might also be an explanation for the lower incidence in IVD-related diseases in female dogs.

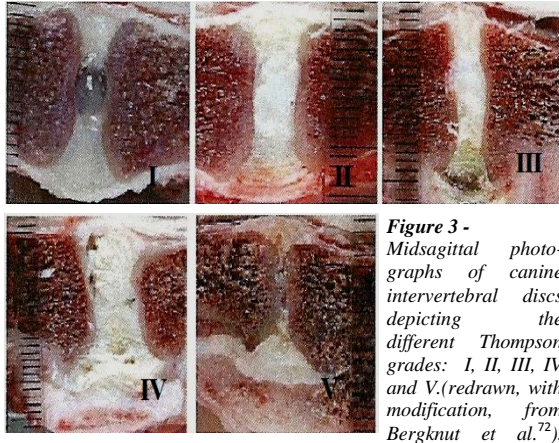
Dogs that are highly predisposed to IVD-related diseases are mainly chondrodystrophic (CD). Chondrodystrophy implies disturbance of the endochondral ossification resulting in characteristic disproportionate short curved legs, a phenotypically feature that has been favoured in selective breeding programs<sup>59,60</sup>. As a consequence, CD dogs can be phenotypically, radiographically and histologically, distinguished<sup>39,61-66</sup> from non-chondrodystrophic (NCD) breeds. Examples of CD dogs are the Basset Hound, Drever, Scottish Terrier, French Bulldog, Shi Tzu, Pomeranian, Pug, Whels Corgi, and similarly the Dachshund, miniature Poodle, Pekingese, Beagle, Lhasa Apso, and the Cocker Spaniel<sup>12</sup>. In particular, it has been shown that Beagles serve as proper animal models for spontaneous IVD degeneration in studying human disease, since these dogs have shown many similarities with humans in morphological appearance, histological structure, and biochemical characteristics in the different stages of IVD degeneration<sup>15</sup>.

Several studies support that CD breeds are at greater risk and are more prone to disc degeneration than NCD breeds<sup>5,24,36,41</sup>. Therefore, it is assumed that there might be a correlation between the genetic factors of chondrodystrophy and IVD degeneration, which are probably closely linked<sup>12</sup>. But this still remains unproven and only genetic research would be helpful. In NCD breeds IVD degeneration also occurs, although to a significant lesser extent<sup>67</sup>. In these dogs a multifactorial etiology, especially trauma and wear and tear<sup>39,68</sup>, is more likely<sup>23</sup>. However, in some of these NCD breeds IVD-related diseases are also overrepresented<sup>12</sup>, suggesting a genetic association as well. The most common NCD breeds that are affected by IVD degenerative diseases include the German Shepherd, Doberman, Rottweiler, and the Labrador Retriever<sup>69,70</sup>, but for these breeds also applies that evident genetic relations with IVD degeneration remains still unknown and thus require additional research.

The process of degeneration is macroscopically characterized by a gradual shift from a mucoid translucent gray NP, towards a non-translucent white NP, accompanied by the loss of the annular-nuclear demarcation, the emergence of focal disruptions, cleft formation and a significantly reduce in the IVD space<sup>39,71</sup>. To distinguish these different stadia of the degeneration process, Bergknut et al. (2011)<sup>72</sup> validated the human grading scheme to grade gross



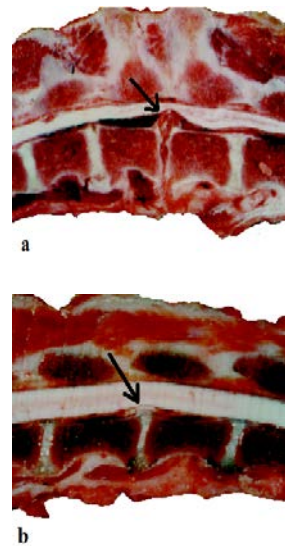
macroscopic pathological changes by Thompson et al. (1990)<sup>71</sup>, in dogs. The scheme consists of five major categories, ranging from completely healthy, to severely extensive degenerated IVDs, in consecutive numerical order, respectively (see figure 3)<sup>71</sup>. Secondary consequences of the process, such as herniation of the IVD, are not included in the grading scheme.



**Figure 3 -** Midsagittal photographs of canine intervertebral discs depicting the different Thompson grades: I, II, III, IV and V. (redrawn, with modification, from Bergknut et al.<sup>72</sup>).

The fundamental pattern of the entire above-described degenerative process is similar in both CD and NCD dog breeds<sup>23,39</sup>, and therefore the Thompson grading scheme can be applied in both affected CD and NCD dog breeds<sup>71,72</sup>. The most important differences in the IVD degeneration between these CD and NCD breeds are the age of onset and progression of the degenerative changes<sup>23,39</sup>. The process of IVD degeneration among CD breeds usually starts earlier in life (<1 year)<sup>13,39,73</sup> and proceeds very rapidly, while the less frequently affected NCD breeds generally show more gradually degenerative signs at significantly later ages (>6 years)<sup>39,73</sup>. Another existing distinctive feature in degenerating IVDs between CD and NCD breeds, is the common mineralization of the NP in CD breeds<sup>23,39,74-76</sup>. This deposit of minerals is secondary to tissue necrosis<sup>39</sup>, and is very rarely observed in NCD dogs. The calcification alters the biomechanical loading of the IVD and may have an impact on the degeneration process and its ultimate pathological end-stage. Whereas a degeneration process without mineralization is associated with a gradual collapse of the NP, a calcified NP is sturdier in retaining the disc height. Therefore, in calcifying degenerative discs it corresponding takes longer before the AF also starts to degenerate<sup>39,68</sup>, but because the calcified NP in the meantime significantly falls short in its function as hydraulic shock-absorbing cushion, the AF suddenly will be exposed to extra workload. The speed of the degenerative course among CD breeds, and the corresponding sudden exposure of the AF to an increased workload, in these dogs often leads to explosive Hansen type I

herniations (AF rupturing), whereas the more gradual degenerative weakening course of all disc components in NCD breeds leads to gradual Hansen type II herniations, with inefficient responding, bulging, and eventual nerve-compressing annular fibers<sup>39,68</sup>. If Hansen type I herniations occur in NCD dogs a much smaller amount of NP material needs to be extruded from the vertebral canal compared to the amount of mineralized material in a CD dog (figure 4)<sup>39,68</sup>.



**Figure 4 -** Photographs of severe type I (a) and II (b) herniations in necropsy specimens from a five-year-old Beagle (CD-breed) and a nine-year-old Border Collie (NCD-breed), respectively. The upper photograph (a) shows complete failure of the AF, with nerve-compressing extruded calcified nuclear material (arrow). The photograph below (b) shows an IVD with a nerve-compressing bulging AF and a less hydrated NP. Note the absence of obvious degenerative changes in adjacent IVDs of the Border Collie (b) and conversely the multiple affected degenerated and calcified IVDs in the Beagle (a) (redrawn, with modification, from Bray and Burbridge<sup>68</sup>).

At last, the spinal location and the number of affected IVDs are also different in CD and NCD dog breeds. IVD degeneration in CD dogs usually affects multiple IVDs (figure 4), which are mostly localized in the cervical and thoracolumbar area<sup>13,39</sup>. In contrast, degenerative alterations in NCD breeds are usually limited to one IVD (figure 4), which is mostly in the lower cervical or lumbar area<sup>39,51,69,70</sup>. These IVDs are more mobile and are generally exposed to greater workload, which suggests that IVD degeneration in NCD dogs is predominantly caused by trauma or wear and tear<sup>23</sup>.

Altogether, differences in age, progression, predisposed location, and mineralization, but similarities in the fundamental degenerative process, suggest an etiological distinction between these two types of dog breeds. In CD dogs a genetic cause seems to be more likely whereas in NCD dogs this seems to be a multifactorial cause.

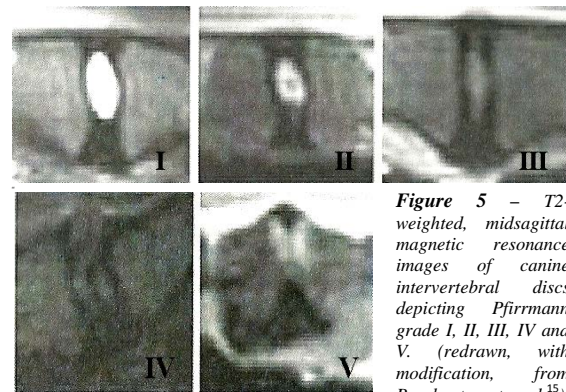
## Diagnosis

Nowadays, IVD degeneration and the potential ensuing problems in dogs, is being detected more and more<sup>5,12-14,24,54,77</sup>. The current increasing incidence is partly correlated with an increased occurrence of this condition in canine populations. One explanation is the increase in



popularity of specific dog breeds. Another explanation is the increasingly aging canine population due to the improved overall healthcare of companion animals<sup>24</sup>. However, the increased incidence is also attributable to improved recognition of symptoms by veterinarians, as well as enhanced veterinary diagnostic imaging<sup>24,78</sup>. The diagnosis of IVD disease in dogs is based on the signalment and medical history supplemented by a physical, neurologic and radiographic examination of the animal<sup>77,79,80</sup>. A complete neurologic examination is performed to determine whether neurologic lesions are present and to trace their location(s) and extensiveness in order to list all differential diagnoses, comprising for example vertebral fractures, myelopathies, neuropathies and neoplasia<sup>77,81,82</sup>. The use of diagnostic imaging is indispensable. Applicable imaging techniques include radiography, Magnetic Resonance Imaging (MRI), Computed Tomography (CT), and myelography<sup>83</sup>. Radiography is an easy, inexpensive technique, which does not necessarily require anaesthesia and has except the well-known exposure to radiation minimal side effects. It can be helpful in ruling out diagnoses such as neoplasms and may reveal degenerative processes in the IVD(s)<sup>84,85</sup>. Radiographic findings of degenerative changes in a disc may include signs such as narrowing of the intervertebral space, bulging, herniation, and disc mineralization<sup>86</sup>. The presence of spinal cord compression, however, cannot be confirmed, and radiography lacks in the ability to localize lesions accurately enough<sup>83,86</sup>. Therefore, especially in cases where eventually will be decided to intervene surgically, the use of only radiographic findings is inadequate<sup>83</sup>. For a more accurate view of the localization, site of potential herniations, herniated material and suspected spinal cord compression, the use of myelography, CT or MRI is indicated<sup>83</sup>. Myelography and CT are especially useful for identifying sites of herniation and herniated material, as well as in determining and classifying intradural and extradural spinal cord compressive lesions, respectively<sup>83,87,88,89-92</sup>. Myelography is relatively inexpensive, but complications attributable to the epidural contrast injection such as deterioration of spinal dysfunction, seizing, asystole, and renal failure, are major disadvantages<sup>93-95</sup>. Side effects on the contrast medium are rare in CT, but it is more expensive and requires specialized equipment<sup>83,96</sup>. Nevertheless, radiography with or without contrast and CT are not able to detect subtle early changes suggestive for IVD degeneration<sup>96</sup>. MRI on the other hand is excessively suitable for early recognition and classification of IVD degeneration, due to its ability to demonstrate subtle changes in several tissues<sup>97,98</sup>. This technique utilizes hyperintensity and hypointensity of the NP and AF,

respectively. The signal intensity of the NP on T2-weighted midsagittal MR images is directly correlated with the concentration of water bounded tot proteoglycan, which is high in normal healthy NPs<sup>99</sup>. During the IVD degeneration process, a decrease in signal intensity of the NP is seen on MRI images<sup>83</sup>. The hypointensity of the NP on T2-weighted midsagittal images is correlated to the extent of disc degeneration and Pfirmann et al. (2001)<sup>100</sup> have developed a widely used MRI-based grading system for human IVD degeneration<sup>96-102</sup>. The system is based on the earlier mentioned Thompson grading scheme<sup>71,100</sup>, and is validated by Bergknut et al. (2010)<sup>67</sup> in dogs. This grading scheme can be applied in living animals, and can be used to assessing degenerative changes. The five distinguishable stadia in the Pfirmann grading scheme of T2-weighted midsagittal MR images, vary from a homogenous, bright white and hyperintense NP with clear distinctions between the NP and AF and a normal disc height (grade I), to an inhomogeneous, black, hypointense NP with lost distinction between the NP and AF and a collapsed disc space (grade V)<sup>100</sup>. The different grades in dogs are presented in figure 5<sup>15</sup>.



**Figure 5** – T2-weighted, midsagittal magnetic resonance images of canine intervertebral discs depicting Pfirmann grade I, II, III, IV and V. (redrawn, with modification, from Bergknut et al.<sup>15</sup>).

By combining the midsagittal views with sagittal and transverse MR images, detailed information of the IVD(s) can be obtained, concerning possible degeneration, bulging, protrusion, and/or extrusion<sup>39,97,98</sup>. Furthermore, surrounding structures such as the ligaments and spinal cord can be assessed as well<sup>103</sup>. Disadvantages of the use of MRI are the high costs and the limited availability in veterinary practice<sup>82</sup>. Distinction between pathological degeneration and normal age-related changes can be challenging<sup>43</sup>.

### Therapy and Prognosis

The diversity and severity of clinical manifestations among patients with IVD degeneration mainly determine the choice of treatment and accompanying prognosis. The patient's breed, age, lifestyle, symptoms, and potential concomitant medical problems, as well as the willingness of the owner are therein decisive.



The choice of treatment is either conservative or surgical. Typical conservative medical interventions in cases of IVD disease include the systemic use of analgesic and anti-inflammatory drugs (NSAIDs), combined with an initially controlled and limited physical activity<sup>83</sup>, and later, an overall change of lifestyle whereby jumping, running, playing and slippery floors should be avoided. Controlled and limited physical activity initiate healing of the injured area, and a combination of physical therapy and a quiet lifestyle is helpful in diminishing potential physical discomfort<sup>90,104-110</sup>. Acupuncture is sometimes also labelled as pain relieving method<sup>111,112</sup>, although evidence is lacking. In case of muscle spasms, muscle relaxants can be very useful, and in addition the urinary bladder function can pharmacologically be managed by Alfa-adrenergic antagonists or cholinergic agonists, depending on the affected neural structures<sup>83,113</sup>. It is important that during conservative treatment both owner and clinician frequently observe the patient for potential progression or worsening, because signs may suddenly worsen and cause irreversible damage to neural tissues<sup>22</sup>. Successful outcomes of conservative management are not very convincing, and vary from 40 to 50%<sup>114-116</sup>. Recurrence after successful treatment is common. Some studies report recurrence rates of more than one third of all initially successfully conservatively treated dogs<sup>117,118</sup>. In dogs that do not respond to conservative management surgical intervention is indicated.

Surgical management is specifically advisable in IVD patients with ataxia, motor deficits or nonresponsive, progressive, or severe symptoms such as nonambulatory paraparesis. Both surgery and the ensuing postoperative care require specific knowledge, specialized equipment, skilled competences, time, and careful attention in order to achieve desired outcomes. Surgical procedures are essentially aimed at decompression of neural tissue and the removal of degenerated and extruded disc material. Common decompressive procedures are hemilaminectomy, pediclectomy, dorsal laminectomy, and a ventral slot procedure<sup>22,77,83,119,120</sup>. In hemilaminectomy parts of the vertebral lamina, pedicle and articular facets are unilaterally removed. Pediclectomy includes the removal of pedicular bone but preserves these articular facets, and the dorsal laminectomy involves the removal of the dorsal spinous process and dorsal vertebral lamina<sup>69,83</sup>. The ventral slot procedure approaches the discs ventrally and can only be applied in the cervical region, and therefore is not feasible in thoracolumbar IVDs<sup>22,69,83</sup>. Extruded disc material can more easily be removed by performing hemilaminectomy rather than a dorsal

laminectomy<sup>22,69,119,121</sup>, but increases the risk of venous sinus haemorrhage. On the other hand hemilaminectomy is less invasive, is less time consuming and shows better postoperative results<sup>69,83,121</sup>. Pediclectomy can be applied as an adjunctive technique in those cases where a bilateral approach to the vertebral canal is desired, and is the quickest and least invasive procedure with the slightest influence on the stability of the vertebral column, followed by the hemilaminectomy and dorsal laminectomy<sup>69,121</sup>. For that reason, the pediclectomy and hemilaminectomy sometimes can be extended over a few more discs in a row<sup>77,80,83</sup>. The surgical consideration concerning different procedures particularly depends on differences in invasiveness, the access to extruded disc material, the side and degree of spinal root compression and the possible influences on the stability of the vertebral column. Prognostic outcomes of decompressive surgical interventions are very diverse, and complicate prediction of consistent surgical results<sup>69,83</sup>. Factors such as the absence or presence of deep pain perception, invasiveness of the surgical procedure, potential complications, duration and severity of clinical symptoms, the rate of disappearance of symptoms after surgery, and the use of different criteria for a successful outcome all appear to contribute to a greater or lesser extent<sup>22,69,122,123</sup>. For instance, patients with intact deep nociception have better successful surgical outcomes than patients without<sup>83</sup>, and cervical decompressive surgery displays better results than thoracolumbar decompressive surgery<sup>69</sup>. Because of the divergent surgery results surgical intervention should be a deliberate choice and therewithal does not solve the problem of the degenerating discs. In some cases it might alleviate some pain but there also exist fair chances of no improvement, recurrence, or even worsening.

Taken into account that current therapies aim at alleviating pain and symptoms and principally do not solve the problem of the degenerative process, there is a strong need for innovative therapies that intervene or reverse the processes of IVD degeneration. Smolders et al. (2012) examined a surgical partial disc replacement by a novel nucleus pulposus prosthesis (NPP) in situ<sup>124</sup>. The ability of the NPP to restore disc functionalities showed promising results, however in almost half of the cases fragmentation/herniation of the NPP occurred and therefore improvement of the concept and NPP properties remains required. In human medicine new methods are being investigated with emphasis and special interest in biological cell based therapies. With the implantation of cells alone or in conjunction with specific genes, these experimental methods focus





on the pathophysiological process of IVD degeneration and are primarily aimed at cellular repair of the degenerating disc matrix<sup>25</sup>. However, these techniques are still far from imaginable clinical applications. Delivery of the genes is technically difficult, conditions in degenerated discs may not be favorable enough for survival of implanted cells, and the correct choice of cells and genes requires more research, knowledge and improved understanding concerning the pathogenesis of IVD degeneration<sup>25</sup>.

In the context of the repeatedly addressed strong needs for more research towards IVD degenerative disorders, prostaglandin E2 (PGE2) is proposed to have impact on the disc matrix. In the subsequent section the background of PGE2 and its possible role within the processes of degeneration will be outlined. Thereafter, the research to establish the most reliable ELISA for quantifying PGE2 in canine IVD material shall be discussed. Beagles were included in the study, and as stated, these CD-dog breeds have shown to be valid translational models for research on human IVD degeneration<sup>15</sup>.

## Prostaglandin E2

### Origin and background

Along with tromboxanes and leukotrienes, the prostaglandins belong to the eicosanoids. These molecules derive from either  $\omega$ -3 or  $\omega$ -6 essential fatty acids (EFAs) and perform a very wide range of physiological functions in lots of different organ systems. The principal bioactive prostaglandins are prostacyclin (PGI<sub>2</sub>), prostaglandin D<sub>2</sub> (PGD<sub>2</sub>), prostaglandin F<sub>2 $\alpha$</sub>  (PGF<sub>2 $\alpha$</sub> ) and PGE<sub>2</sub>. Each of these different prostaglandins has its own major task, and the differences in expression of enzymes within cells determine the profile of prostaglandin production<sup>125</sup>. For example, activated mast cells predominantly produce PGD<sub>2</sub>, while activated macrophages mainly synthesize PGE<sub>2</sub>. PGE<sub>2</sub> is one of the most abundant and widely characterized prostaglandin in animal species<sup>125</sup>. Under physiological circumstances this molecule regulates various cell types and contributes to many different body systems including for example the immune response, blood pressure, uterus contractility, gastrointestinal and bronchial smooth muscles, central and peripheral nerves, and in addition gastric acid and gastric mucus secretion. Prostaglandins and in particular PGE<sub>2</sub> also play a major role in the inflammatory response. Damage of a cell membrane induces the activation of the membrane-bound enzyme phospholipase A<sub>2</sub> by which the  $\omega$ -6 EFA arachidonic acid is released. Consecutively, directed by the main pro-

inflammatory cytokines IL-1 and TNF- $\alpha$ , arachidonic acid is mainly converted by the damage-induced and released cyclooxygenase (COX) type 2 isoenzymes into prostaglandins<sup>125</sup>. PGE<sub>2</sub> is involved in all processes leading to the classic inflammatory signs such as rubor, calor, edema and pain and is therefore considered as a major inflammatory mediator<sup>126</sup>. At first, it acts on peripheral sensory neurons and central sites within the spinal cord and the brain, and is associated with sensitization of proprioceptive neurons and involved in pain induction. In addition, it effectuates arterial dilatation and increases the microvascular permeability, resulting in redness, warmth, and edema<sup>125,126</sup>. To limit inflammation, pharmacological interventions of inflammatory pathways hinder the prostaglandin production by interrupting the arachidonic acid cascade. This can be established either by inhibition of phospholipase A<sub>2</sub> or cyclooxygenase enzymes via the use of corticosteroids and NSAIDs respectively. Based upon this mechanism, current treatments in patients with intervertebral disc disease involve the use of NSAIDs as well. Glucocorticoid administration should be avoided because of the major side effects<sup>127,128</sup>. To limit the NSAID side effects, especially selective COX-2 inhibitors such as Celecoxib should be used, and furthermore it is advised to limit their use to 3 months. By means of relieving spinal pain and counteracting associated inflammatory responses, this symptomatic approach in degenerative disc diseases may improve the patient's quality of life<sup>127,128</sup>.

### Prostaglandin E2 and intervertebral disc degeneration

Miyamoto et al. (2006) have shown that mechanical stress in disc cells increases PGE<sub>2</sub> levels<sup>129</sup>, and there are multiple studies that have shown increased amounts of inflammatory agents in degenerative IVDs, including PGE<sub>2</sub><sup>130-132</sup>. According to a study performed by O'Donnell (1996) in symptomatic herniated human lumbar disc specimens, extruded discs generally tended to be associated with higher PGE<sub>2</sub> content than protruded ones<sup>133</sup>. The increased quantities of PGE<sub>2</sub> levels are attributed to cellular responses sequentially on the damage that is caused during stress or the degenerative process, and the mediators derive from the local cell population as well as from invading cells. The presence and reported increased levels within the IVDs might suggest a potential role of PGE<sub>2</sub> in disc metabolism and the degenerative processes in IVD patients. Miyamoto et al. (2002) have described a possible role of PGE<sub>2</sub> in IVDs in pain or hyperalgesia. It is suggested that PGE<sub>2</sub> is associated with sensitization of proprioceptive neurons and act on pain-inducing



substances such as bradykinin<sup>134</sup>. In mice, Reinold et al. (2005) have demonstrated that the absence of PGE2 receptors of the EP2 receptor subtype results in the lack of spinal hyperalgesia after administering inflammatory stimuli, which implies that spinal inflammatory hyperalgesia is mediated by prostaglandin E receptors of the EP2 subtype<sup>135</sup>. This might be important in both canine and human low back pain problems as well, although concrete evidence is lacking. Eventually the PGE2 elevations in the aforementioned studies should be interpreted with certain prudence as well, because these studies were all performed in vitro and therewithal in different cell populations and materials (e.g. herniated or non-herniated material).

There is little research on PGE2 in the IVD, particularly in contrast to PGE2 roles in articular cartilage. The cartilage matrix produced by chondrocytes compromise various similarities with the matrix components (e.g. collagen types and proteoglycans) within the NP cells. In the context of the pathophysiology of arthritis, many studies demonstrated diverse mechanisms through which PGE2 acts on chondrocyte metabolism<sup>136-139</sup>. These mechanisms include various roles, such as the induction of chondrocyte apoptosis, inhibition of DNA synthesis and type I collagen gene expression, and on the other hand the stimulation of type II collagen gene expression, the reversal of IL-1 induced proteoglycan degradation, and sensitization of chondrocytes to anabolic action of IGF-1. Particularly because of the similarities between cartilage tissue and matrix components of the NP, it is presumed that these PGE2 actions might also be of importance in the IVD.

In a recent human study from Vo et al. (2010) the possible effects of PGE2 on disc metabolism were examined in more detail<sup>140</sup>. In isolated NP tissues from patients that underwent surgical procedures for degenerative but non-herniated IVDs, the expression of key matrix structural genes, as well as the expression of arachidonic acid cascade components responsible for the prostaglandin production were determined by using microarray analysis. In a semiquantitative RT-PCR the effects of PGE2 on the gene expression of key matrix structural genes, enzymes, proteoglycans, growth factors and collagens were measured. Important enzymes involved in IVD remodeling and degeneration are the matrix metalloproteinases (MMPs). Breakdown of collagen type I and II fibers is effected by MMP-1 and MMP-2 respectively and in turn, inhibition of these MMPs is accomplished by anti-catabolic tissue inhibitors of metalloproteinases (TIMPs)<sup>23</sup>. Although some studies report that inflammation may possibly accelerate degenerative processes by the up-regulation of MMPs<sup>131,141,142</sup>, one of the

results in the study was that PGE2 slightly decreased mRNA for MMP-1, and in addition COX-2 inhibition reduced the IL-1 mediated suppression of proteoglycan synthesis. On the other hand common COX inhibitors are able to significantly diminish the proteoglycan synthesis<sup>143</sup>, and taken together, these findings consequently might suggest that endogenously produced prostaglandins support matrix proteoglycan synthesis, which would implicate a potential indirect physiological regulatory role of PGE2 in disc matrix homeostasis.

However, findings from Vo et al. also infer that PGE2 might fulfill negative roles within the disc. In their study inflammatory induced PGE2 elevations by TNF- $\alpha$  significantly decreased disc proteoglycan synthesis and down-regulated the production for both collagen type I and II. Furthermore, mRNA expression for the anti-catabolic factor TIMP-1 and anabolic factor IGF-1 were decreased. Altogether, the elevated catabolic effects and increased breakdown of important structural disc components by PGE2 suggest a potential negative impact on the disc matrix homeostasis. The in vitro reported increased amounts of PGE2 in degenerative IVDs therefore could play a role in the pathophysiology of in vivo IVD degeneration. In that case NSAIDs may not only have analgesic potency in IVD degeneration, but may also impact disc metabolism by eliminating the catabolic effect on the disc cells.

Aforementioned data suggest that principal cell types of the IVD might be either positively or negatively affected by PGE2, but it should be noted that these data were obtained under different conditions with variable materials (e.g. NP cells from herniated or non-herniated IVDs). Furthermore, in vivo research lacks, but possibly could provide more knowledge and understanding regarding the role of PGE2 in IVD degeneration.

## Aim of the study

This study is a part of the Bio Medical Materials (BMM) program and is part of the IDiDAS project, which stands for: Intervertebral Disc diseases, Drug delivery and Augmentation through smart Polymeric biomaterials. Within this program hydrogels and microspheres have been developed that are able to generate a slow release of a drug. In this study two types of hydrogels and microspheres were loaded with a selective COX-2 inhibitor (Celecoxib, CXB) and injected intradisally to accomplish a reduction in the PGE2 content in the IVD. Biosafety and biocompatibility were evaluated positively in mice before using the controlled release systems in dogs. The PGE2



content of all lumbar NPs was determined and the effect of loaded and unloaded controlled release systems was compared to a bolus injection of CXB. To determine PGE2 levels, two types of PGE2 ELISAs were tested. Because results were not consistent in test materials, this study was designed to establish the most reliable ELISA. In order to preserve the valuable canine test material bovine material was used. The output of this research will be decisive for the choice of the ELISA to be used in the canine in vivo experiment.

## Materials and Methods

### Tissue collection

In figure 6 the different steps of tissue collection are displayed (I-VIII). Bovine IVDs were collected from two fresh cow tails (indicated as CT1 and CT2) obtained from slaughterhouse Van Kooten in Montfoort (I). The materials were processed in the same way as the canine IVDs in the in vivo experiment. After a gross dissection of overlying muscles, tendons and fat (II), the tail vertebrae were transversally cut with a band saw halfway through the vertebral bodies (III). The separate IVD units were stored on dry ice (-79°C), and transported to the Division of Surgical Specialties of the Department of Orthopaedics, at the University Medical Center of Utrecht. Subsequently, the IVD units were cut in the sagittal plane using a 0.1 mm diamond saw, in order to prevent material waste as a result of sawing (IV). On each of the resultant two equal parts of each IVD one vertebral body half was removed with a blade No. 11, and the remaining parts were wrapped in aluminum foil and placed in liquid Nitrogen (-196°C). Until further analysis, materials were frozen and stored at -70°C. Subsequently, 60µm tissue sections were obtained at the Department of Biochemistry and Cell Biology at the Faculty of Veterinary Medicine in Utrecht, by using the Leica CM 350 Cryostat. The IVD units were fixated by placing the bony parts of the tissue in Optimal Cutting Temperature (O.C.T.) Tissuetek (V) and subsequently were sectioned and collected on MLS Knittel Glaser microscopy slides. Each microscopy slide contained approximately 3 tissue sections (VI) and was placed on dry ice until the entire IVD was sectioned. Thereafter, the NP and AF were separated on each microscopy slide with blades No. 11 and No. 10 respectively (VII), and in turn separately collected in their corresponding Eppendorf tubes both containing 500µl Ambion® lysis buffer, which is certified RNase-free (VIII). Cut remnants were placed back in the aluminum foil and along with the labeled Eppendorf tubes frozen and stored at -70°C. Because of another ongoing research on gene expression, all materials

were gathered RNase-free. For this study only the CT1 sample material was used for analysis.



**Figure 6** – The different steps of tissue collection. From cow tail to supernatant (I-VIII), which is required for the BCA and ELISAs.

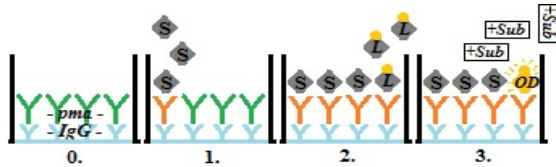
### BCA Protein quantification

To be able to compare the PGE2 levels of NPs from different size IVDs, these were corrected for total protein content by using the Thermo Scientific Pierce® BCA protein Assay Kit. This test principally utilizes the biuret reaction, which is the reduction of  $\text{Cu}^{2+}$  to  $\text{Cu}^{1+}$  by protein in an alkaline medium. By administering a reagent containing bicinchoninic acid (BCA), eventually a purple-colored reaction product is formed by the chelation of two BCA molecules with one cuprous cation ( $\text{Cu}^{1+}$ ). This colorimetric detection of protein concentration is determined with reference to standards of bovine serum albumin (BSA). In order to obtain an average impression of protein quantities as well as to preserve supernatant for the ELISAs, several aliquots of the supernatant of the collected bovine NPs were created and a number of these were pooled and applied in the BCA. The test was performed according to the manufacturer's instructions. From the two assay procedures that are presented, the Microplate Assay Procedure with sample to working reagent ratio 1:20 was performed since it requires smaller volumes of protein sample. Working range was limited to 125-2000µg/mL and absorbance was measured at 540nm after 30 minutes incubation at 37°C. A measure of goodness of fit ( $r^2$ ) was calculated for the BCA standard curve. The  $r^2$  range from 0.0-1.0 and summarizes the discrepancy between observed and expected values under the curve. The more  $r^2$  approaches 1.0, the better X lets you predict Y which means the curve fits better. Standard curves with  $r^2$  values above 0.98 are generally accepted as reliable.



**PGE2 ELISAs**

To quantify the PGE2 levels in the samples, PGE2 ELISA kits manufactured by R&D Systems and ENZO Life Sciences were available. Both R&D and ENZO assays are based on a forward sequential competitive binding technique (see figure 7), in which PGE2 present in the sample (S) competes with horseradish peroxidase-labeled PGE2 (L) for a limited amount of binding sites on the PGE2 monoclonal antibodies (pma) that are bound to anti-mouse IgG (IgG) precoated 96-well plates (0). The sample PGE2 is allowed to bind first (1), then labeled PGE2 (2) and its substrate (+Sub (3)) are administered, and eventually there is an inverse relationship between the optical density (OD) and the amount of PGE2 in the sample.



**Figure 7** – Forward sequential competitive binding. 0: binding PGE2 monoclonal antibodies (pma) to anti-mouse IgG precoated wells; 1: binding PGE2 sample (S); 2: binding labeled PGE2 (L); 3: addition of substrate (+Sub). The resulting optical density (OD) is inversely related to the amount of PGE2 in the sample.

The different ELISA's were performed according to the manuals. To attain the required amounts of supernatant bovine NP sample aliquots were pooled and consecutively applied in both assays. The R&D and ENZO assays range from 39.1-2500 pg/mL, and the sensitivity of the R&D is 30.9 pg/mL, compared to 13.4 pg/mL of the ENZO. These and other specific details such as the cross-reactivity of the different ELISAs are summarized in table 1. The absorbance rates (A) of the R&D were measured using the microplate reader set to 450nm with wavelength correction set to 540nm. For the ENZO they were read at 405nm with wavelength correction set to 595nm. Standard curves were plotted, each corresponding  $r^2$  was calculated, samples were performed in duplicate and to identify whether the PGE2 detection was affected by the biological sample matrix, spike-and-recovery experiments with spikes of 250pg/mL PGE2 were performed in duplicate. Relative standard deviations (SD%) or Coefficients of Variability (CV) were expressed and the quantified PGE2 concentrations in the native samples were related to the corresponding total protein concentrations from the BCA. All results were calculated by Microplate Manager® (MPM) 6 Software, and the outcomes of the different ELISAs were compared.

This research project primarily focusses on the selection of the most reliable ELISA, and therefore repeatability of the assay results is the most important outcome parameter. By testing samples with greater numbers of replicates, more insight will be obtained in the intra-assay precision

(IAP). The IAP is an average value for all of the replicates of a sample in the same assay and reflects the performance of the ELISA in the hands of the user<sup>144</sup>. For the IAPs of the R&D and ENZO 1:8, 1:16 and 1:32 sample dilutions were applied six times. The variable which expresses plate to plate consistency is called the inter-assay precision. Intra- and inter-assay coefficients of variability less than 10 and 15, respectively, are generally acceptable<sup>144</sup>. The IAPs and inter-assay values for the different assays are illustrated in table 1.

	R&D	ENZO	HS
<b>Sensitivity</b>	30.9pg/ml (39.1-2500pg/mL)	13.4pg/ml (39.1-2500pg/mL)	8.26pg/ml (7.8-1000pg/mL)
<b>Intra-assay CV% (&lt; 10%)</b>			
[Low PGE2]	9.0	8.9	9.8
[Medium PGE2]	5.0	5.8	6.1
[High PGE2]	6.1	17.5	3.1
<b>Inter-assay CV% (&lt; 15%)</b>			
[Low PGE2]	12.9	3.0	12.1
[Medium PGE2]	9.9	5.1	12.6
[High PGE2]	9.0	3.9	8.1
<b>Cross-reactivity</b>	PGE3 14.5%	PGE1 70%	PGE1 70%
	PGF2α 7.6%	PGE3 16.3%	PGE3 16.3%
	PGF1α 7.4%	PGF1α 1.4%	PGF1α 1.4%
	PGE1 5.3%	PGF2α 0.7%	PGF2α 0.7%
	6kPGF1α 4.2%	6kPGF1α 0.6%	6kPGF1α 0.6%
	PGA2 0.55%	PGA2 0.1%	PGA2 0.1%
	others <0.1%	PGB1 0.1%	PGB1 0.1%
		others <0.1%	others <0.1%

**Table 1** – Specific details of the R&D, ENZO and ENZO-HS ELISAs. Intra- and inter-assay coefficients of variability less than 10 and 15, respectively, are generally acceptable.

As will be addressed in the results and discussed further in the discussion, at a certain point during the experiment inconsistent bovine assay results eventually have led to the implementation of canine test material in both the R&D and ENZO assays as well as the introduction of a more sensitive third ELISA: the ENZO High Sensitivity (ENZO-HS). The ENZO-HS is based on the same principle as the other two ELISA's, but the assay ranges from 7.8-1000pg/mL and has a sensitivity of 8.26 pg/mL. The specific details of the ENZO-HS compared to the other assays are also listed in table 1. Both canine and bovine samples were applied in the ENZO-HS. Supernatant of the pooled sample of nine dogs was applied in all three ELISAs and in all assays a new pooled bovine NP sample mix ('Bmix2-U') from the remaining cryoslides was applied, since there was not enough supernatant left from the first undiluted bovine pooled sample ('Bmix1-U'). From the canine material similar ELISA/BCA variables were measured as stated for the bovine, but in addition, in all three ELISAs a second dilution series was added and positive and negative control samples were applied by the in vitro stimulation of cells with TNF-α and an intended 56°C PGE2 heat destruction for 20 minutes, respectively. Absorbance rates of the ENZO-HS were measured at 405nm with wavelength correction set to 595nm. In the BCA aliquots of a pooled homogenized



canine NP sample from nine dogs were used. The undiluted sample ('Cmix-U') was applied in six replicates, and dilution series till 1:16 were completed in duplicate. At last, a second ENZO-HS was performed to measure low concentrations. All results were compared in order to select the most reliable test which will be used for the further research of canine material.

## Results

All references to the tables and figures concerning the results (*tables 2-12* and *figures 8-14*) refer to the appendices (**Appendix A**: list of result tables and **Appendix B**: list of result figures).

### BCA Protein quantification

The outcomes of the dilution standards with its standard deviations (SDs) and coefficients of variability (CV) rates are displayed in *table 2* and the corresponding standard curve is shown in *figure 8*. CV(%) is the relative SD which is defined as the SD of a set of measurements divided by their corresponding mean, and is multiplied by 100 to express the outcomes in percentages. The  $r^2$  of the standard curve was calculated at 0.999. The results of the undiluted bovine pooled sample ('Bmix1-U') are shown in *table 3*. The total protein concentration in the pooled bovine mix at 1221.57 $\mu$ g/mL.

### PGE2 ELISAs

The results of the R&D and ENZO dilution standards are shown in *table 4*. The corresponding standard curves are shown in *figure 9* and *figure 10*. Sample results of both the R&D and ENZO have been displayed in *table 5*. Unfortunately in both assays antibodies were erroneously pipetted in the NSB wells.

The R&D PGE2 standard curve ranged from 0.244-0.573 (manual: 0.257-1.319), while the ENZO PGE2 standard curve ranged from 0.049-0.510 (manual: 0.052-0.516). The  $r^2$  of both the R&D and ENZO standard curves is 1.000. The SDs of the sample dilutions are lower in the ENZO kit compared with the R&D kit. Furthermore, the R&D intra-assay precision (IAP) in the 1:8, 1:16 and 1:32 sample dilutions with  $n = 6$ , had mean concentrations of 135.21pg/mL, 212.385pg/mL and 140.081pg/mL and standard deviation rates of 79.36%, 22.12% and 72.28% respectively. The ENZO IAP results were 14.934pg/mL, 17.505pg/mL and 13.019pg/mL, with standard deviations of 21.52%, 21.72% and 14.43%.

The ENZO spiked samples showed standard deviations from 0.00%, 3.00% and 2.38% for the 1:8, 1:16 and 1:32 dilutions, compared to 51.61%, 52.47% and 59.29% for the R&D.

The PGE2 concentrations of the undiluted NP pooled bovine sample in the R&D and ENZO assays were calculated at 61.105pg/mL and 33.914pg/mL, respectively. As shown in *table 6*, related to total protein concentrations from the BCA, the R&D PGE2/total protein is (61.105pg/mL) / (1221.57  $\mu$ g/mL) = 0.050pg/ $\mu$ g. For the ENZO the PGE2/total protein was calculated at (33.914pg/mL) / (1221.57 $\mu$ g/mL) = 0.028pg/ $\mu$ g.

### Canine Results: BCA

Total protein in intervertebral disc material from the in vivo experiments in beagle dogs was applied in the same BCA assay plate as the bovine material. Therefore, dilution standards and the corresponding standard curve ( $r^2=0.999$ ) are identical, and shown in *table 2* and *figure 8*, respectively. The dilution results of the pooled homogenized canine NP sample are presented in *table 7*. The total protein concentration in the undiluted pooled homogenized canine NP sample was 565,438 $\mu$ g/mL. Standard deviation in the 1:2 dilutions was 4.56%, compared to 50.92% in the 1:16 dilutions.

### Canine Results: ELISA's

The results of the R&D, ENZO, and ENZO-HS dilution standards are shown in *table 8*. Their corresponding standard curves are displayed in *figure 11*, *figure 12* and *figure 13*. Because of a double applied amount of conjugate the calibration line of the ENZO dilution standards was performed in mono. Therefore, the outcomes of the ENZO dilution standards in *table 8* do not contain means, SDs and CVs. The standard curves of the R&D, ENZO and ENZO-HS ranged from 0.253-0.630 (manual: 0.257-1.319), 0.004-0.446 (manual: 0.052-0.516) and 0.073-1.004 (manual: 0.061-0.889), respectively. The  $r^2$  of the R&D standard curve was 0.998, compared to 0.999 for the ENZO and 0.992 for the ENZO-HS. The R&D, ENZO and ENZO-HS sample results are organized together in *table 9*. The additional dilution series (2500-39pg/mL) are indicated with 'AdS', and the samples that were heated to 56°C to achieve PGE2 destruction are indicated with '°C-PGE2' and served as a negative control.

In *table 9*, the IAP results are included in the multiple replicates of the 1:2 till 1:16 dilutions. The undiluted ENZO-HS sample comprises the lowest CVs. The AdS showed that in the R&D the lower PGE2 concentrations (78pg/mL and 39pg/mL) are outside the range of the standard curve, while in the ENZO-HS higher PGE2 concentrations (2500pg/mL and 1250pg/mL) could not be measured. CVs of lower AdS concentrations (313pg/mL and 156pg/mL) in the R&D were 47.84% and 61.01%, compared to 1.7% and 11.8%



of the ENZO, and 7.71% and 19.11% of the ENZO-HS. The standard deviations of the R&D spike values ranged from 25.07%-44.41%. Likewise, the ENZO spike CVs ranged from 3.48%-31.98%, and the ENZO-HS from 3.14%-18.73%. The undiluted TNF- $\alpha$  samples in the R&D, ENZO and ENZO HS kit were above the range of the standard curve and could not be measured reliably. The 56°C heat-treated samples had absorbance rates of 0.661, 0.44 and 1.63 in the R&D, ENZO and ENZO-HS, respectively. The PGE2 concentrations corrected for the total protein content of the canine sample dilutions and the Bmix2-U are summarized in *table 10*.

The results of the second ENZO-HS that was performed to measure low concentrations are shown in *table 11* (dilution standards), *figure 14* (standard curve), and *table 12* (sample results). The standard curve from the second performed ENZO-HS ranges from 0.084-1.020 (manual: 0.061-0.8889) and had an  $r^2$  of 0.999. The associated CVs range from 1.90% to 14.29%, and PGE2 concentrations in all performed Bmix2 dilutions were too low (high absorbance rates) for measurable ranges.

## Discussion

Degeneration of intervertebral discs (IVDs) is an important and common cause of back problems in both humans and dogs. Current available therapies are not able to arrest or reverse the process and consequently a strong need to clarify the exact mechanisms of the process remains. This study examined the possible role of prostaglandin E2 (PGE2) in IVD degeneration. Beagles were intradiscally injected with controlled release systems of Celecoxib (CXB) to accomplish a reduction of PGE2, and the effect of both loaded and unloaded controlled release systems was compared to a bolus injection of CXB. To determine the PGE2 content within the different IVDs three different ELISAs were tested. The goal of this study was to select the most reliable ELISA to measure PGE2 content in the IVDs from Beagles enrolled in the *in vivo* study. Bovine material was included to preserve the valuable canine test material.

The IVDs of the gathered cow tails did not have gel-like NPs. In literature it is described that discs from cows above 15 months of age do not have notochordal cells anymore, and that the disappearance of these probably disc maintaining cells is correlated with early degenerative changes<sup>145</sup>. Therefore, it is not inconceivable that judging from just the macroscopic image the bovine discs would have been degenerative. From both cow tails that were collected only one cow tail

(CT1) could be used as sample material in the different assays due to the sawing process. Instead of straight sagittal cuts through the IVDs, the NPs of CT2 repeatedly slipped along the 0.1 mm diamond saw resulting in unequal IVD parts containing either the complete NP, or lacking it. One explanation could be the loss of tension of the saw band during the process. Other explanations for the unequal divided IVD could be the fixation angle, as well as the speed and force that was used to push the sample through the saw. Furthermore, the nature of the NPs of the CT2 sample material might have been more compliant, due to differences in hydration.

During the Cryostat and the separation procedure of the NP and the AF, blood vessels were carefully excluded, since plasma levels of PGE2 could influence the PGE2 determinations of the NP sample materials. As O.C.T. Tissuetek® could interfere with PGE2 measurements, half of the IVD units were fixated in the Cryostat with their bony parts embedded into the O.C.T. Tissuetek®. The largest IVD unit of CT1 was technically the most difficult one to cut up in the Cryostat. Because of its height, size and weight, the contact surface to the Tissuetek (O.C.T.) was too small to properly fixate the whole IVD unit during cutting. Thus, this IVD repeatedly slipped to the bottom of the Cryostat, where it came in contact with tissue waste and Tissuetek (O.C.T.). The polyethylene glycol (PEG) component of O.C.T. has the ability to destabilize membrane bilayers<sup>146</sup> and may be cytotoxic<sup>147</sup>. Because of this and the probability of contact with vertebral bone and cartilage remnants in the tissue waste, the supernatant of this IVD was not used in this study, since both could interfere with PGE2 measurements.

As is apparent in the BCA results, the standard curve (*figure 8*) fits very well ( $r^2$  of 0.999) and the absorbance rates approached expected ratios as diluted down the plate. However, when observing the canine results of *table 7*, the replicates in the higher sample dilutions were less accurate, up to a CV of 50.92% in the 1:16 dilutions. This greater variation specifically in the higher dilutions might be declared by buffer disturbances. The canine samples were diluted in the lysis buffer, and it is known that buffers often contain several substances (such as PEG) that might interfere with the performance of an assay<sup>148</sup>. The PGE2 levels corrected for total protein (*table 10*) in these dilutions therefore should be interpreted carefully. To obviate this in the sequel, it is recommended to perform additional tests concerning the influence of the applied buffer. Differences in the performed BCA duplicates might be caused by inefficient vortexing, resulting in an inhomogeneous sample. Vortexing was performed



for 30 seconds with a shake speed of approximately 500 rpm. Possibly, next time it would be better to vortex longer and at a higher speed. To ensure liquid is retained within the wells at higher speeds, sealing the plate during shaking might be helpful. Nevertheless, in the undiluted samples the pooled bovine sample evidently shows a greater total protein amount (1221.57 $\mu$ g/mL) compared to the undiluted pooled canine sample (46.513 $\mu$ g/mL), with both comparable SDs. Because in this study there have not been any correction for material weight, the most logical explanation for the higher protein levels in the bovine NPs can be attributed to the larger amount of sample material that was put in the bovine pooled sample. Therefore, the lack of material weight correction can be denoted as a limitation of this study.

In the bovine ELISA results, both standard curves (*figure 9* and *figure 10*) have a reliable fit. However, it is noticeable that the curve range of the R&D corresponds less with the manual range, especially compared with the ENZO in which the curve comprises quite the same range as prescribed. The R&D assay range is evidently a lot smaller than expected. The resulted smaller range cannot be declared by the difference in duplicates. It is however more likely that this might be influenced by for example the buffer, which might interfere to a greater extent within the R&D assay. Another possibility would be the instability of PGE2 due to the repeatedly processes of defrosting and freezing, in between the different performed tests. In the literature it is known that in human plasma and serum a significant reduction in the levels of the majority of lipid metabolites (including arachidonic acid) is achieved when subjected to repeated freeze-thaw cycles<sup>149</sup>. Consequently, as a well-known derivate of arachidonic acid, PGE2 might also be sensitive for possible degradation of metabolization during the repeated process of freeze-thawing. When comparing the duplicates of the standard dilutions in both assays, the R&D shows higher deviations in the absorbance rates (*table 4*). Standard general assay aspects such as pipetting technique, intermingling between wells, remaining wash buffer or procedural errors such as an uneven plate coating are not very likely to contribute as main causes of duplicate variation in this study. More samples are aberrant through the whole assay and in this case it is more plausible that the difference in duplicate deviations might be explained by intra-assay characteristics. It is therefore certainly more plausible that this might be initiated by for example interference with buffer components as well. The higher CV results in the R&D dilution standards affect the results of the bovine samples. As shown in the PGE2/BCA results (*table 6* and *table 5*) the ENZO repeatedly measured lower PGE2 amounts

in both the undiluted and diluted material of the same pooled bovine sample. The higher concentrations found in the R&D might be associated with the obtained smaller standard curve range in the R&D. If the range of the assay is smaller, the distinctive capacity becomes smaller, and only small differences in absorbance, can result in high differences in calculated values.

As expected, the values of the BLANK duplicates and the TA of the ENZO were respectively low and high. However, the NSB results of both R&D and ENZO were high, while in the absence of antibodies these values are expected to be very low. During the experiment antibodies had erroneously been pipetted in the NSB wells, resulting in unreliable NSB results. In addition, the duplicates of the spiked samples in the R&D assay showed high variations, which was most likely also due to a human error. It is however certain that these values are unreliable for further calculations. For the other spikes within the ENZO the duplicates were more constant, and the SDs were markedly lower than in the R&D.

The B<sub>0</sub> in the R&D had high ODs, and that is what was expected in this sample, that does not contain PGE2. Compared with the dilution standards, the B<sub>0</sub> in the ENZO assay is also high, but values in the 1:2 sample dilution, and for example also the 1:4 sample mean absorbance rate exceeded the zero standard. However, the 1:2 and 1:4 sample duplicates had CV rates of respectively 86,51% and 125,2% with associated concentration values that are lower than the lowest standard (39pg/mL). These values therefore cannot be interpreted and a logical explanation would be that the bovine samples contain very low PGE2 concentrations. Literature concerning specific PGE2 quantities in bovine IVDs is limited. The most representative study to compare our data with is from Van Dijk et al. (2013)<sup>150</sup>. In this study, a sustained release of CXB was tested in a bovine in vitro model of extruded herniation. Before treated with CXB, several cultured bovine NP tissue explants were exposed to lower osmotic conditions to initiate swelling, an inflammatory response and simulate extruded herniation. An ENZO ELISA assay was used to determine PGE2 release over time and quantities were normalized to original sample weight. As a control one experimental group was not treated with CXB and the cultured bovine tissue explants were surrounded by an artificial AF to prevent swelling. In the measurements of these NPs the maximum average PGE2 concentration over time was 1.3 pg/mL/mg tissue. In *table 5*, the ENZO concentration of the undiluted bovine sample is 33.914pg/mL with a CV of 9.45%. However, it is very difficult to compare these values because sample conditions are not



completely equal, and moreover, in this study the samples were not weighed which makes both quantities very difficult to interpret.

Most striking is that in both assays the PGE2 concentrations actually do not decrease in the several dilutions (including the spikes) and therewithal show inconsistency. Especially in the R&D the duplicates had noticeable high CVs and the sample dilution concentrations are far from consistent. In the 1:8 and higher dilutions, including the 1:64, all PGE2 values were inconsistent and remarkably higher than the undiluted sample. In the ENZO the differences between the dilutions and the undiluted sample were somewhat less prominent, but especially in the lower ranges of this assay the PGE2 concentrations did not decrease as well as the sample is diluted down the plate. Problems especially seems to manifest in the diluted samples. The samples were diluted in the buffer that they were lysed in, and buffer interference might be responsible for the increasing inconsistency specifically within the higher dilutions. Here also applies, that further buffer experiments are recommendable. Both assays run from 39pg/mL to 2500pg/mL, and numerous sample concentration values fell outside these assay ranges. These values are out of range for the sensitivity of the assays which might also indicate that the bovine samples have very low levels of PGE2 present. In succession, for more accurate measurements it can be necessary to use extraction procedures as described in both assay manuals. Nevertheless, when considered together, the bovine R&D and ENZO results both demonstrated their instabilities. In general the ENZO was somewhat more consistent than the R&D and mostly comprises lower deviations, but a lot of samples were not within the measurable range and both assays have shown that the results of the bovine sample dilutions appeared to be unpredictable. The IAP values show that especially in the lower concentrations of the R&D, but also in the ENZO, the SDs and CVs were very high and because all of this, there is eventually decided to insert a third ELISA: the ENZO-HS. This ELISA is according to the manufacturer more sensitive (see also *table 1*) and can measure a range from 7.8-1000pg/mL. Because of the low PGE2 levels in the bovine material, canine material was introduced in all three ELISAs, in order to select the most reliable ELISA.

For all three assays in *table 8* the  $r^2$  is within the acceptable value. Therefore, the fitted standard curves (*figure 11*, *figure 12* and *figure 13*) can be denoted as reliable. The AdS of the ENZO (*table 9*) looks consistent: duplicates are performed well and the linearity of the dilutions is fairly constant. Compared to the other two ELISAs, the

ENZO AdS results comprises the smallest CVs and were the most steady in multiple dilutions. The R&D particularly showed high SD rates for AdS concentrations below 313pg/mL and the PGE2 could not be measured for both lowest AdS concentrations (78pg/mL and 39pg/mL) because both values were outside the range of the standard curve. For the same reason, the PGE2 levels of the two highest AdS concentrations (2500pg/mL and 1250pg/mL) appeared to be immeasurable for the ENZO-HS, and the first measurable high AdS concentration (625pg/mL) in the ENZO-HS had a very large SD (106.75%). Associated outcomes were demonstrated in the sample results. The canine R&D sample and IAP results were comparable with the outcomes of the bovine ELISAs, since it also illustrated the unpredictability and instability of the dilution series. Again, except for the 1:2 dilution, R&D dilution values demonstrated higher PGE2 concentrations than in the undiluted sample. For the canine ENZO this was not the case, but PGE2 concentrations starting from the 1:4 dilution were all beneath the curve range, and consequently the ENZO lacked the capacity to measure below the 1:2 dilutions. Despite the ENZO standard curve was performed in mono, it is likely that these results can be interpreted as reliable, since the ODs look similar to the earlier performed assay. These findings rather suggest that canine samples contain low levels of PGE2 as well. Like the canine ENZO, the canine ENZO-HS also showed expected decreased PGE2 levels in the several dilutions, but on the other hand this assay was also able to quantify PGE2 concentrations in the lower assay ranges, up to the 1:8 dilution series. Thus, together with the AdS outcomes this confirms that the R&D is especially less consistent in the lower range, and that the ENZO-HS is capable of detecting relatively low PGE2 levels in the canine discs.

Medium of cells stimulated with TNF- $\alpha$  to produce PGE2, served as a positive control in the PGE2 quantification assays. In the TNF- $\alpha$  wells of all assays, the expected low absorbance rates and corresponding high PGE2 amounts were measured. With most deviations beneath the desired 10% (*table 1*), in both the ENZO and ENZO-HS the TNF- $\alpha$  replicates were performed accurately, especially in comparison with the R&D (*table 9*) with CVs up till 90.20%. In the ENZO-HS most of the TNF- $\alpha$  absorbance rates were low, and thus PGE2 amounts were higher than the highest PGE2 standard. Concerning the negative control, only the ENZO-HS demonstrated expected outcomes. As stated in literature, PGE2 has a very short half-life time under physiological conditions and it is assumed that elevated temperatures might result in thermal decomposition<sup>151</sup>. After the intended twenty-minute 56°C PGE2 heat destruction in the





samples, in the ENZO-HS the PGE2 amount was lower than in the corresponding undiluted sample results. This suggests that the intended PGE2 heat destruction should have been successfully. However, remarkably enough the PGE2 levels in the R&D and ENZO after the sample heat treatment were even higher than their corresponding undiluted sample results. Possibly for these samples the heating time and temperatures were not sufficient enough to achieve PGE2 destruction. The latter is not inconceivable, because in contrast to the known high stability of PGE2 when refrigerated, specific conditions concerning heat resistance of PGE2 have not been investigated so far<sup>151</sup>. On the other hand it is well-known that heat treatment can be responsible for denaturation, membrane destabilization and even cytotoxicity, and in literature it is observed that temperatures above 55°C can alter tissue membrane permeability within two minutes<sup>152</sup>. Therefore, one explanation could be that probably the heat treatment in the R&D and ENZO samples released the PGE2 out of the tissue instead of destructing it, by which in the sequel a longer and/or higher term heat treatment possibly could achieve more impact.

In the spike dilution series, the ENZO-HS 1:4 spike and the ENZO 1:2 spike results were not consistent. At first, the concentrations did not decrease with expected ratios as the spikes were diluted down the plate. Secondly, the duplicates were far apart. With values of respectively 31.98% and 18.73%, the CVs of the ENZO and ENZO-HS both exceeded the acceptable 10%. The latter applies basically for all spikes in the R&D assay, which showed higher CVs than in both the ENZO assays. Consequently the R&D spikes can be reported as the least consistent. For these poor spiking results, the same causes might apply as earlier discussed for the bovine spikes.

Altogether, both the ENZO ELISAs show more consistency than the R&D. However, it is important to take into account the specific ELISA characteristics, as listed in *table 1*. There is a major difference between the cross-reactivity values of the assays. Whereas PGE3 manifests itself as the highest cross-reactivity value (14.5%) in the R&D assay, in both the ENZOs PGE3 cross-reactivity is 16.3%, which is moreover exceeded by 70% PGE1 cross-reactivity. As a result, especially for the ENZOs this means that there might be a considerable chance that PGE2 would be wrongly classified as PGE2, i.e. detected as false positive due to interfering equivalent substances. This might result into a distorted image of PGE2 amounts in the NPs. In literature it is unknown to which extent and in what quantities for example PGE1 is present in bovine and canine (whether or not degenerating) NPs. However, PGE1 is mainly known as an

effective inhibitor of platelet aggregation, acts directly on smooth muscle cells and possesses potent vasodilatory properties<sup>153</sup>. The lack of smooth muscle cells and the non-vascularized nature<sup>23,39</sup> of the NP therefore makes it less likely that substantial PGE1 amounts will be common in the NPs. Yet, because PGE1 is associated with anti-inflammatory properties as well<sup>153</sup>, cautiousness remains necessary when interpreting the results.

The ENZO-HS seem most reliable for comparing the NP PGE2/total protein ratios in both species. Nonetheless, as illustrated in the ENZO-HS ratios in *table 10*, the PGE2 levels demonstrated in both the bovine and canine NPs were relatively low. In order to measure the lower expected PGE2 values and considering the previous ELISA results the second ENZO-HS was performed. The BLANK, TA and B<sub>0</sub> demonstrated typical expected outcomes according to the manufacturer's manual. The assay had very small SDs in a well fitted standard curve and nicely illustrated the amount of slides with the associated PGE2 concentrations. However, the absorbance replicates of the bovine samples unfortunately exceeded the curve range and therefore PGE2 concentrations could not be calculated. Perhaps this might also be explained by a decay of PGE2 due to the repeated freeze-thaw cycles in between all different performed tests<sup>149</sup>.

## Conclusion

The ENZO-HS has shown to be the most reliable PGE2 ELISA for determining PGE2 levels in canine material in future. Bovine and canine NPs appeared to have relatively low PGE2 levels. Reliable measurement of PGE2 levels is crucial in determination of the role of PGE2 in IVD degeneration and development of future therapies, both in humans and in dogs.

## Acknowledgements

Most of all, I would really like to thank N. Willems for her support and supervision of this project. Besides, I would like to mention R. Licht for his assistance in the ELISAs, and J. Wolfswinkel en A.R.J. Bleumink for technical assistance and provision of the Leica CM 350 Cryostat.



## References

1. McNeil JM, Binette J. From the Centers for Disease Control and Prevention. Prevalence of disabilities and associated health conditions among adults. *JAMA* 50:120-125 (2001).
2. Freburger JK, Holmes GM, Agans RP, Jackman AM, Darter JD, Wallace AS, Castel LD, Kalsbeek WD & Carey TS. The rising prevalence of chronic low back pain. *Arch Intern Med* 169:251-258 (2009).
3. Cheung KM, Karppinen J, Chan D, Ho D, Song YQ, Sham P, Cheah KS, Leong JC & Luk KD. Prevalence and pattern of lumbar magnetic resonance imaging changes in a population study of one thousand forty-three individuals. *Spine* 34:943-940 (2009).
4. Maniadas N & Gray A. The economic burden of back pain in the UK. *Pain* 84:95-103 (2000).
5. Gage ED. Incidence of clinical disc disease in the dog. *J Am Anim Hosp Assoc* 135:135-138 (1975).
6. Mooney V. Presidential address. International Society for the Study of the Lumbar Spine. Dallas, 1986. Where is the pain coming from? *Spine* 12:754-759 (1987).
7. Vanharanta H, Guyer RD, Ohnmeiss DD, et al. Disc deterioration in low-back syndromes. A prospective, multi-center CT/discography study. *Spine* 13:1349-1351 (1988).
8. Luoma K, Riihimäki H, Luukkonen R, et al. Low back pain in relation to lumbar disc degeneration. *Spine* 25:487-492 (2000).
9. Webb A. Potential sources of neck and back pain in clinical conditions of dogs and cats: a review. *Vet J* 165:193-213 (2003).
10. Agria I. Five year statistical report. Stockholm (2000).
11. Egenvall A, Bonnett BN, Olson P & Hedhammar A. Gender, age, breed and distribution of morbidity and mortality in insured dogs in Sweden during 1995 and 1996. *Vet Rec* 146:519-525 (2000).
12. Bergknut N, Egenvall A, Hagman R, Gustås P, Hazewinkel HAW, Meij BP, Lagerstedt AS. Incidence and mortality of diseases related to intervertebral disc degeneration in a population over 600,000 dogs. In Bergknut N (ed): *Intervertebral disc degeneration in dogs*, Acta Universitatis Agriculturae Sueciae - doctoral thesis. 91:55-74 (2011).
13. Hoerlein BF. Intervertebral disk protrusions in the dog. I: incidence and pathological lesions. *Am J Vet Res* 14:260-269 (1953).
14. Brown NO, Helpfrey ML, Prata RG. Thoracolumbar disk disease in the dog: a retrospective analysis of 187 cases. *J Am Anim Hosp Assoc* 13:665-72 (1977).
15. Bergknut N, Rutges JPHJ, Smolders LA, Kranenburg HC, Hagman R, Lagerstedt A-S, Grinwis GCM, Voorhout G, Creemers LB, Dhert WJA, Hazewinkel HAW, Meij BP. The dog as a spontaneous animal model for human intervertebral disc degeneration. *Eur Spine J* 19:1399-1400 (2010).
16. Dyce KM, Sack WO, Wensing CJG. The Neck, Back and Vertebral Column of the Dog and Cat, in Dyce KM, Sack WO, Wensing CJG (ed): *Textbook of Veterinary Anatomy* (ed 4), Vol. Philadelphia London New York St. Louis Sydney Toronto, Saunders Elsevier; 407-419 (2010).
17. Case LP. The dog: its behavior, nutrition, and health, 2nd edition, Wiley-Blackwell; 45-46 (2007).
18. Smith BJ: the vertebrae in Smith BJ (ed): *Canine Anatomy*, Wiley-Blackwell; 215-224 (1999).
19. König HE, Liebich HG: Axial skeleton, in König HE, Liebich HG (ed): *Veterinary Anatomy of Domestic Mammals* (ed 4), Schattauer 108-110 (2007).
20. Urban JPG, Roberts S, Ralphs JR. The Nucleus of the Intervertebral Disc from Development to Degeneration. *Oxford Journals Life Sciences Integrative and Comparative Biology* 40:53-61 (2000).
21. King AS, Smith RN. A comparison of the anatomy of the intervertebral disc in dog and man: with reference to herniation of the nucleus pulposus. *Br Vet J* 3:135-49 (1955).
22. Toombs JP, Waters DJ: Intervertebral Disc Disease in Slatter DH (ed): *Textbook of small animal surgery*, Elsevier Health Sciences; 1193-1209 (2003).
23. Bergknut N. Intervertebral disc degeneration in dogs, Acta Universitatis Agriculturae Sueciae - doctoral thesis general Introduction; 91:18-53 (2011).
24. Bray JP, Burbridge HM. The Canine Intervertebral Disk. Part One: Structure and Function. *Journal of the American Animal Hospital Association* 34:55-63 (1998).
25. Urban JPG and Roberts S. Degeneration of the intervertebral disc. *Arthritis Res Ther* 5:120-130 (2003).
26. Hendry NGC. The hydration of the nucleus pulposus and its relation to intervertebral disk derangement. *J Bone Joint Surg* 40:132-43 (1958).
27. White AA, Panjabi MM. Clinical biomechanics of the spine. JB Lippincott, Philadelphia; 1-42 (1978).
28. Johnson EF, Caldwell RW, Berryman HE, et al. Elastic fibers in the annulus fibrosus of the dog intervertebral disc. *Acta Anat (Basel)* 118:238-242 (1984).
29. Coventry MB. Anatomy of the intervertebral disk. *Clin Orthop* 67:9-15 (1969).
30. Ghosh P, Bushell GR, Taylor TKF, Akeson WH. Collagens, elastin and non-collagenous protein of the intervertebral disk. *Clin Orthop* 129:124-9 (1977).
31. Kapandji IA. The physiology of the joints. (ed 2). Edinburgh: Churchill-Livingston 3:564-91 (1974).
32. Evans JM, Barbenel JC. Structural and mechanical properties of tendon in relation to function. *Eq Vet J* 7:1-8 (1975).
33. Hukins DWL. Disc Structure and Function, in Ghosh P (ed): *The Biology of the Intervertebral Disc* (ed 1), Boca Raton, Florida, CRC Press, 1:1-38 (1988).
34. Roughley PJ. Biology of intervertebral disc aging and degeneration: involvement of the extracellular matrix. *Spine* 29:2691-2699 (2004).
35. Setton LA, Chen J. Mechanobiology of the intervertebral disc and relevance to disc degeneration. *J Bone Joint Surg Am* 2:52-57 (2006).
36. Ghosh P, Taylor TK, Braund KG. The variation of the glycosaminoglycans of the canine intervertebral disc with ageing. I. chondrodystrophoid breed. *Gerontology* 23:87-98 (1977).
37. Slijper EJ. Comparative biologic-anatomical investigations on the vertebral column and spinal musculature of mammals. *Proc K ned Adak wet Verh* 47:1-128 (1946).
38. Hildebrand M. Analysis of vertebrate structure. New York: Wiley, 1-710 (1974).
39. Hansen HJ. A pathologic-anatomical study on disc degeneration in dogs, with special reference to the so-called enchondrosis intervertebralis. *Acta Orthop Scand Suppl* 11:1-117 (1952).
40. Ghosh P, Taylor TK, Braund K, et al. A comparative chemical and histochemical study of the chondrodystrophoid and nonchondro-dystrophoid canine intervertebral disc. *Vet Pathol* 13:414-427 (1976).
41. Ghosh P, Taylor TK, Braund KG. Variation of the glycosaminoglycans of the canine intervertebral disc with ageing. II. Non-chondrodystrophoid breed. *Gerontology* 23:99-109 (1977).
42. Ghosh P, Taylor TK, Braund K, et al. The collagenous and non-collagenous protein of the canine intervertebral disc and their variation with age, spinal level and breed. *Gerontology* 22:124-134 (1976).
43. Adams MA, Roughley PJ. What is intervertebral disc degeneration, and what causes it? *Spine* 31:2151-2161 (2006).
44. Knutsson F. The instability associated with disk degeneration in the lumbar spine. *Acta Radiol* 25:593-609 (1944).
45. Coventry MB, Ghormley RK, Kernohan JW. The intervertebral disk: its microscopic anatomy and physiology. Part II: changes in the intervertebral disk concomitant with age. *J Bone Joint Surg* 27:233-247 (1945).
46. Butler D, Trafimow JH, Andersson GBJ, McNeill TW, Huckman MS. Disks degenerate before facets. *Spine* 15:111-113 (1990).
47. Jonck LM. The mechanical disturbances resulting from lumbar disk narrowing. *J Bone Joint Surg* 43:362-75 (1961).
48. Kahmann RD, Butterman GR, Lewis JL, Bradford DS. Facet loads in the canine lumbar spine before and after disk alteration. *Spine* 15:971-978 (1979).
49. Adams MA, Dolan P, Hutton WC, Porter RW. Diurnal changes in spinal mechanics and their clinical significance. *J Bone Joint Surg* 72:266-270 (1990).
50. Postacchini F, Gumina S, Cinotti G, Perugia D, DeMartino C. Ligamenta flava in lumbar disc herniation and spinal stenosis. Light and electron microscopic morphology. *Spine* 19: 917-922 (1994).
51. da Costa RC, Parent JM, Partlow G, et al. Morphologic and morphometric magnetic resonance imaging features of Doberman Pinschers with and without clinical signs of cervical spondylomyelopathy. *Am J Vet Res* 67:1601-1612 (2006).
52. Jones JC, Inzana KD. Subclinical CT abnormalities in the lumbosacral spine of older large-breed dogs. *Vet Radiol Ultrasound* 41:19-26 (2000).
53. Buckwalter JA. Aging and degeneration of the human intervertebral disc. *Spine* 20:1307-1314 (1995).
54. Priestler WA. Canine intervertebral disc disease - Occurrence by age, breed, and sex among 8,117 cases. *Theriogenology* 6:293-303 (1976).
55. Goggin JE, Li A, Franti CE. Canine intervertebral disk disease. Characterization by age, sex, breed and anatomic site of involvement. *Am J Vet Res* 31:1687-92 (1970).
56. Walker TL, Gage DE, Selcer RR. Disorders of the spinal cord and spine of the geriatric patient. *Vet Clin N Am Sm Anim Pract* 11:765-786 (1981).
57. Smolders et al. Canonical Wnt Signaling in the Notochordal Cell is Upregulated in Early Intervertebral Disk Degeneration. *Journal of orthopaedic research*. 30:950-957 (2011).
58. Calleja-Agius J, Muscat-Baron Y, Brincat MP. Estrogens and the intervertebral disc. *Menopause Int.* 3:127-30 (2009).
59. Vans HE, Christensen GC: Joints and Ligaments, in Evans HE, Christensen GC (ed): *Miller's Anatomy of the Dog* (ed 2), Philadelphia London Toronto, WB Saunders Company; 225-268 (1979).
60. Olsson SE, Hansen HJ. Cervical disc protrusions in the dog. *J Am Vet Med Assoc* 121:361-370 (1952).
61. Beachley MC, Graham FH Jr. Hypochondroplastic dwarfism (enchondral chondrodystrophy) in a dog. *J Am Vet Med Assoc* 163:283-284 (1973).
62. Johnson KA. Skeletal Diseases. In: Ettinger SJ, Feldman EC, (ed). *Textbook of veterinary internal medicine*. (ed 6). Philadelphia: Saunders Co. 1965-1991 (2005).
63. Bingel SA, Sande RD. Chondrodysplasia in five great Pyrenees. *JAVMA* 205:845-848 (1994).
64. Breur GJ, Zerbe CA, Slocombe RF, et al. Clinical, radiographic, pathologic, and genetic features of osteochondrodysplasia in Scottish deerhounds. *JAVMA* 195: 606-612 (1989).
65. Bingel SA, Sande RD. Chondrodysplasia in the Norwegian elkhound. *Am J Pathol* 107:219-229 (1982).



66. T. Koide, H. Katayama, Y. Sumi and K. Ishi. A case of new chondrodystrophy. *Pediatr Radiol* 13:102-105 (1983).
67. Bergknut N, Auriemma E, Wijsman S, Voorhout G, Hagman R, Lagerstedt AS, Hazewinkel HAW, Meij BP. Pfirrmann grading of intervertebral disc degeneration in chondrodystrophic and non-chondrodystrophic dogs with low-field magnetic resonance imaging. In Bergknut N(ed): Intervertebral disc degeneration in dogs. Acta Universitatis Agriculturae Sueciae - doctoral thesis 91:75-91 (2011).
68. Bray JP, Burbridge HM. The Canine Intervertebral Disk. Part Two: Degenerative changes – nonchondrodystrophoid versus chondrodystrophoid disks. *Journal of the American Animal Hospital Association* 34:135-144 (1998).
69. Brisson BA. Intervertebral disc disease in dogs. *Vet Clin North Am Small Anim Pract* 40:829-858 (2010).
70. Meij BP, Bergknut N. Degenerative lumbosacral stenosis in dogs. *Vet Clin North Am Small Anim Pract* 40:983-1009 (2010).
71. Thompson JP, Pearce RH, Schechter MT, et al. Preliminary evaluation of a scheme for grading the gross morphology of the human intervertebral disc. *Spine* 15:411-415 (1990).
72. Bergknut N, Grinwis G, Pickee E, Auriemma E, Lagerstedt AS, Hagman R, Hazewinkel HA, Meij BP. Reliability of macroscopic grading of intervertebral disk degeneration in dogs by use of the Thompson system and comparison with low-field magnetic resonance imaging findings. *Am J Vet Res*.72:899-904 (2011).
73. Braund KG, Ghosh P, Taylor TK, et al. Morphological studies of the canine intervertebral disc. The assignment of the beagle to the achondroplastic classification. *Res Vet Sci* 19:167-172 (1975).
74. Melrose J., Burkhardt, D., Taylor, T.K., Dillon, C.T., Read, R., Cake, M., Little, C.B. Calcification in the ovine intervertebral disc: a model of hydroxyapatite deposition disease. *Eur. Spine J.* 18:479-489 (2009).
75. Stigen O. Calcification of intervertebral discs in the dachshund: an estimation of heritability. *Acta Vet Scand* 32, 197-203 (1991).
76. Stigen O, Christensen, K. Calcification of intervertebral discs in the dachshund: an estimation of heritability. *Acta Vet Scand* 34, 357-361 (1993).
77. Hoerlein BF: Intervertebral disks. In Hoerlein BF (ed): *Canine Neurology* (ed 3), Philadelphia, WB Saunders; 470-560. (1978).
78. Suwankong, N. Voorhout, G. Hazewinkel, HA, and Meij, BP. Agreement between computed tomography, magnetic resonance imaging, and surgical findings in dogs with degenerative lumbosacral stenosis. *J Am Vet Med Assoc*, 229:1924-1929. (2006).
79. DeLahunta A: *Veterinary Neuroanatomy and Clinical Neurology*; Philadelphia, WB Saunders; 169-220 (1977).
80. Shores A. The intervertebral disk syndrome in the dog: Part I. Pathophysiology and management. *The Compendium on Continuing Practicing Veterinarian* 3:639-643 (1981).
81. Withrow SJ. Localization and diagnosis of spinal cord lesions in small animals (Part I). *Compend Contin Educ Pract Vet* 2:464. (1980).
82. Griffin JF, Levine JM, Kerwin SC. Canine Thoracolumbar Intervertebral Disk Disease: Pathophysiology, Neurologic Examination, and Emergency Medical Therapy. *Compendium: Continuing Education for Veterinarians*. [http://cp.vetlearn.com/Media/Publications/Article/PV0309\\_WEB\\_Griffin\\_IVD\\_D1\\_CE\\_0.pdf](http://cp.vetlearn.com/Media/Publications/Article/PV0309_WEB_Griffin_IVD_D1_CE_0.pdf) (2009).
83. Griffin JF, Levine JM, Kerwin SC, Cole RC. Canine Thoracolumbar Intervertebral Disk Disease: Diagnosis, Prognosis and Treatment. *Compendium: Continuing Education for Veterinarians*. <http://www.2ndchance.info/limping-Griffin2009Intervertebraldisk.pdf> (2009).
84. Bartels JE, Hoerlein BF, Boring JG: *Neuroradiography*. In Hoerlein BF (ed): *Canine Neurology*, (ed 3), Philadelphia, WB Saunders; 103-135 (1978).
85. Morgan JP. *Radiology in Veterinary Orthopedics*. Lea & Febiger (ed), Philadelphia; 219-300 (1972).
86. Lamb CR, Nicholls A, Targett M, et al. Accuracy of survey radiographic diagnosis of intervertebral disc protrusion in dogs. *Vet Radiol Ultrasound* 43:222-228 (2002).
87. Ferreira AJA, Correia JHD, Jaggy A. Thoracolumbar disc disease in 71 paraplegic dogs: influence of rate of onset and duration of clinical signs on treatment results. *J Small Anim Pract* 43:158-163 (2002).
88. Cudia SP, Duval JM. Thoracolumbar intervertebral disk disease in large, nonchondrodystrophic dogs: a retrospective study. *JAAHA* 33: 456-460 (1997).
89. Drost WT, Love NE, Berry CR. Comparison of radiography, myelography and computed tomography for the evaluation of canine vertebral and spinal cord tumors in sixteen dogs. *Vet Radiol Ultrasound* 37:28-33 (1996).
90. Coates JR. Intervertebral disk disease. *Vet Clin North Am Small Anim Pract* 30:77-110 (2000).
91. Olby NJ, Dyce J, Houlton JEF. Correlation of plain radiographic and lumbar myelographic findings with surgical findings in thoracolumbar disc disease. *J Small Anim Pract* 35:345-350 (1994).
92. Olby NJ, Munana KR, Sharp NJH, et al. The computed tomographic appearance of acute thoracolumbar intervertebral disc herniations in dogs. *Vet Radiol Ultrasound* 41:396-402 (2004).
93. Allan GS, Wood AKW. Lohexol myelography in the dog. *Vet Radiol Ultrasound* 29:78-82 (1988).
94. Carroll GL, Keene BW, Forrest LJ. Asystole associated with iohexol myelography in a dog. *Vet Radiol Ultrasound* 38:284-287 (1977).
95. Widmer WR, Blevins WE. Veterinary myelography: a review of contrast media, adverse effects, and technique. *JAAHA* 27:163-177 (1991).
96. Modic MT, Masaryk TJ, Ross JS, et al. Imaging of degenerative disk disease. *Radiology* 168:177-186 (1988).
97. Besalti O, Pekcan Z, Sirin YS, et al. Magnetic resonance imaging findings in dogs with thoracolumbar intervertebral disk disease: 69 cases. *JAVMA* 228: 902-908 (2006).
98. Pfirrmann CW, Dora C, Schmid MR, et al. MR image-based grading of lumbar nerve root compromise due to disk herniation: reliability study with surgical correlation. *Radiology* 230:538-588 (2004).
99. Pearce RH, Thompson JP, Bebault GM, et al. Magnetic resonance imaging reflects the chemical changes of aging degeneration in the human intervertebral disk. *J Rheumatol* 27:42-43 (1991).
100. Pfirrmann CW, Metzendorf A, Zanetti M, Hodler J, and Boos N. Magnetic resonance classification of lumbar intervertebral disc degeneration. *Spine* 26:1873-1878 (2001).
101. Kettler A, and Wilke HJ. Review of existing grading systems for cervical or lumbar disc and facet joint degeneration. *Eur Spine J.* 15:705-718 (2006).
102. Wilke HJ, Rohlmann F, Neidlinger-Wilke C, Werner K, Claes L, and Kettler A. Validity and interobserver agreement of a new radiographic grading system for intervertebral disc degeneration: Part I. Lumbar spine. *Eur Spine J* 15:720-730. (2006).
103. Ito D, Matsunaga S, Jeffery ND, et al. Prognostic value of magnetic resonance imaging in dogs with paraplegia caused by thoracolumbar intervertebral disk extrusion: 77 cases. *JAVMA* 227:1454-1460 (2005).
104. Edge-Hughes L. Conservative management of chondrodystrophic dogs with thoracolumbar intervertebral Disc Disease (IVDD). *CHAP Newsletter*, 4-6 (2007).
105. Michlovitz SL. *Thermal Agents in Rehabilitation*. (F.A. Davis Company: Philadelphia, PA (1990).
106. Moses PA. Module 1: Small Animal Neurology. In: *Pathological Conditions in Animals 1*. (Copyright the University of Queensland) (2006).
107. Scremin AM, Kurata L, Gentili A et al. Increasing muscle mass in spinal cord injured persons with a functional electrical stimulation exercise program. *Arch Phys Med Rehabil*. 80:1531-1536 (1999).
108. Vallani C, Carcano C, Piccolo G et al. Postural pattern alterations in orthopaedics and neurological canine patients: postural evaluation and postural rehabilitation techniques. *Vet Res Comm*. 28:389 – 391 (2004).
109. Kathmann I, Demierre S, Jaggy A. Rehabilitation methods in small animal neurology. *Schweiz Arch Tierheilkd*. 143:495-502 (2001).
110. Hoerlein BF. Further evaluation of the treatment of disc protrusion paraplegia in the dog. *JAVMA* 129:495-502 (1956).
111. Scavelli TD, Schoen A. Problems and complications associated with the nonsurgical management of intervertebral disc disease. *Probl Vet Med* 1:402-414 (1989).
112. Janssens LA, DE Prins EM. Treatment of thoracolumbar disk disease in dogs by means of acupuncture: a comparison of two techniques. *JAAHA* 25:169-174 (1989).
113. Trotter EJ: *Canine intervertebral disc disease*. In Kirk RW (ed): *Current Veterinary Therapy VI*, Philadelphia, WB Saunders; 844 (1977).
114. Funkquist B. Thoraco-lumbar disk protrusion with severe cord compression in the dog. II. Clinical observations with special reference to the prognosis in conservative treatment. *Acta Vet Scand* 3:317-343 (1962).
115. Funkquist B. Decompressive laminectomy in thoraco-lumbar disc protrusion with paraplegia in the dog. *J Small Anim Pract* 11:445-451 (1970).
116. Wilcox KR. Conservative treatment of thoracolumbar intervertebral disc disease in the dog. *JAVAM* 147:1458-1460 (1965).
117. Hoerlein BF: Intervertebral disc disease. In Oliver JE, et al (ed): *Veterinary Neurology* WB Saunders, Philadelphia; 32 (1987).
118. Russel SW, Griffiths RC: Recurrence of cervical disc syndrome in surgically and conservatively treated dogs. *J Am Vet Med Assoc* 153:1214 (1968).
119. Smith GK, Walter MC. Spinal decompressive procedures and dorsal compartment injuries: Comparative biomechanical study in canine cadavers. *Am J Vet Res* 49:266 (1988).
120. Trotter EJ: Dorsal laminectomy for treatment of thoracolumbar disc disease. In Bojrab MJ (ed): *Current Techniques in Small Animal Surgery*, (ed 3). Lea & Febiger, Philadelphia; 608 (1990).
121. Gage ED, Hoerlein BF. Hemilaminectomy and dorsal laminectomy for relieving compressions of the spinal cord in the dog. *J Am Vet Med Assoc* 152:351-9 (1968).
122. Griffiths IR. Vasogenic edema following acute and chronic spinal cord compression in the dog. *J Neurosurg*. 42:155-65 (1975).
123. Olsson SE. The dynamic factor in spinal cord compression: a study on dogs with special reference to cervical disc protrusion. *J Neurosurg* 15:308-321 (1958).
124. Smolders LA et al. Biomechanical evaluation of a novel nucleus pulposus prosthesis in canine cadaveric spines. *The Veterinary Journal*, 192:199-205 (2012).
125. Ricciotti E, FitzGerald GA. Prostaglandins and inflammation. *Arterioscler Thromb Vasc Biol* 31:986-1000 (2011).
126. Funk CD. Prostaglandins and leukotrienes: advances in eicosanoid biology. *Science* 294:1871-1875 (2001).
127. Levine JM, Levine GJ, Johnson SI, Kerwin SC, Hettlich BF, Fosgate GT. Evaluation of the success of medical management for presumptive thoracolumbar intervertebral disk herniation in dogs *Vet Surg*. 36:482-491 (2007).



- 128.** Levine JM, Levine GJ, Johnson SI, Kerwin SC, Hettlich BF, Fosgate GT. Evaluation of the success of medical management for presumptive cervical intervertebral disk herniation in dogs *Vet Surg.* 36:492-499 (2007).
- 129.** Miyamoto H, Doita M, Nishida K, et al. Effects of cyclic mechanical stress on the production of inflammatory agents by nucleus pulposus and annulus fibrosus derived cells in vitro. *Spine* 31:4-9 (2006).
- 130.** Kang JD, Georgescu HI, McIntyre-Larkin L, Stefanovic-Racic M, Evans CH. Herniated lumbar intervertebral discs spontaneously produce matrix metalloproteinases, nitric oxide, interleukin-6, and prostaglandin E2. *Spine* 21:271-17 (1996).
- 131.** Kang JD, Stefanovic-Racic M, McIntyre LA, Georgescu HI, Evans CH. Toward a biochemical understanding of human intervertebral disc degeneration and herniation. Contributions of nitric oxide, interleukins, prostaglandin E2, and matrix metalloproteinases. *Spine* 22:1065-73 (1997).
- 132.** Willburger RE, Wittenberg RH. Prostaglandin release from lumbar disc and facet joint tissue. *Spine* 19:2068-70 (1994).
- 133.** O'Donnell JL, O'Donnell AL. Prostaglandin E2 content in herniated lumbar disc disease. *Spine* 21:1653-1655 (1996).
- 134.** Miyamoto H, Saura R, Doita M, Kurosaka M, Mizuno K. The role of cyclooxygenase-2 in Lumbar Disc Herniation. *Spine* 27:2477-2483 (2002).
- 135.** Reinold H, Ahmadi S, et al. Spinal inflammatory hyperalgesia is mediated by prostaglandin E receptors of the EP2 subtype. *J Clin Invest* 115:673-9 (2005).
- 136.** Amin AR, Dave M, Attur M, et al. COX-2, NO, and cartilage damage and repair. *Curr Rheumatol Rep* 2:447-453 (2000).
- 137.** Goldring MB, Berenbaum R. The regulation of chondrocyte function by proinflammatory mediators; prostaglandins and nitric oxide. *Clin Orthop Relat Res* 427:37-46 (2004).
- 138.** Goldring MB, Suen LF, Yamin R, et al. Regulation of collagen gene expression by prostaglandins and IL-1beta in cultured chondrocytes and fibroblasts. *Am J Ther* 3:9-16 (1996).
- 139.** Riquet FB, Lai W-FT, Birkhead JR, et al. Suppression of type I collagen gene expression by prostaglandins in fibroblasts is mediated at the transcriptional level. *Mol Med* 6:705-719 (2000).
- 140.** Vo NV, Sowa GA, Kang JD, Seidel C, Studer RK. Prostaglandin E2 and Prostaglandin F2 $\alpha$  Differentially Modulate Matrix Metabolism of Human Nucleus Pulposus Cells. *Journal of Orthopaedic research* 28:1259-1266 (2010).
- 141.** Kim JH, Studer RK, Sowa GA, et al. Activated Macrophage-Like THP-1 Cells Modulate Annulus Fibrosus Cell Production of Inflammatory Mediators in Response to Cytokines. *Spine* 33:2253-2259 (2008).
- 142.** Podichetty VK. The aging spine: the role of inflammatory mediators in intervertebral disc degeneration. *Cell Mol Biol (Noisy-le-grand)* 53:4-18 (2007).
- 143.** Yoo JU, Papay RS, Malesud CJ. Suppression of proteoglycan synthesis in chondrocyte cultures derived from canine intervertebral disc. *Spine* 17:221-224 (1990).
- 144.** Inter- and Intra- Assay Coefficients of Variability. [www.salimetrics.com](http://www.salimetrics.com) Salimetrics® Accelerating Salivary Discovery. Spitips; 1-4.
- 145.** Aguiar DJ, Johnson SL, Oegema TR. Notochordal Cells Interact with Nucleus Pulposus Cells: Regulation of Proteoglycan Synthesis. *Experimental Cell Research* 246: 129-137 (1999).
- 146.** Hui SW, Boni LT. PEG effect on lipid bilayers, in Wilschut J, Hoekstra A (eds): *Membrane fusion* (ed 1), Dekker M Inc; 234-239 (1991).
- 147.** Bayliss MT, Urban JP, Johnstone B, Holm S. In vitro method for measuring synthesis rates in the intervertebral disc. *J Orthop Res.* 4:10-17 (1986).
- 148.** Wolfram HM, Siewert S, Rauch P. Limiting cross-reactivity in immunoassays, in: *immunoassay buffer*. [www.aplichem.com](http://www.aplichem.com). Aplichem: 2-9. (2010).
- 149.** Ishikawa M, Maekawa K, Saito K, Senoo Y, Urata M, et al. Plasma and Serum Lipidomics of Healthy White Adults Shows Characteristic Profiles by Subjects' Gender and Age. *PLoS ONE* 9: e91806. doi:10.1371/journal.pone.0091806 (2014).
- 150.** Van Dijk B, Potier E, Van Dijk M, Langelaan M, Keita I. Sustained release of celecoxib reduces prostaglandin E2 production in a novel in vitro model of extruded disc herniation. In Van Dijk(ed): *A physiological in vitro model of intervertebral disc tissue*. Eindhoven University, Ipskamp drukkers BV Enschede – doctoral thesis 73-90 (2013).
- 151.** Watzel B, Zehbe R, Halstenberg S, Kirkpatrick CJ, Brochhausen C. Stability of prostaglandin E2 (PGE2) embedded in poly-D,L-lactide-co-glycolide microspheres: a pre-conditioning approach for tissue engineering applications. *J Mater Sci: Mater Med* 20: 1357-1365 (2009).
- 152.** Bischof JC et al. Dynamics of Cell Membrane Permeability Changes at Supraphysiological Temperatures. *Biophysical Journal* 68: 2608-2614 (1995).
- 153.** Levin G, Duffin KL, et al. Differential metabolism of dihomoc-linolenic acid and arachidonic acid by cyclo-oxygenase-1 and cyclo-oxygenase-2: implications for cellular synthesis of prostaglandin E1 and prostaglandin E2. *Biochem. J.* 365:489-496 (2002).



# Appendices

Used abbreviations:

A	Absorbance rates
AdS	Additional dilution series
B <sub>0</sub>	Zero Standard
BLANK	Background absorbance
CV	Coefficients of variability
°C-PGE2	Heated samples
IAP	Intra-assay precision
NSB	Non-Specific Binding well ( <i>On account of the absence of PGE2-antibodies both the labeled PGE2 as well as sample PGE2 are not able to bind</i> ).
RepliCts	Replicates
r <sup>2</sup>	Measure of goodness of fit. (0.0-1.0)
SD	Standard deviations
TA	Total Activity of the ENZO color reagent.
TNF- $\alpha$	TNF- $\alpha$ stimulated medium
[TP]	Concentration of total protein
/]	Results outside the measuring range
*..*	Values that are not included in further calculations due to very aberrant outcomes.

## Appendix A: list of result tables

Std# ( $\mu\text{g/mL}$ )	RepliCts (A)	Mean (A)	SD (A)	CV %
2000	1.034	1.061	0.038	3.599
	1.088			
1500	0.834	0.881	0.066	7.545
	0.928			
1000	0.596	0.604	0.011	1.758
	0.611			
750	0.501	0.499	0.004	0.709
	0.496			
500	0.382	0.375	0.011	2.832
	0.367			
250	0.234	0.229	0.008	3.404
	0.223			
125	0.181	0.168	0.018	10.943
	0.155			
25	0.104	0.095	0.013	13.398
	0.086			

Table 2 – Results of the BCA dilution standards (std#).

Sample ID	RepliCts (A)	Mean (A)	Conc ( $\mu\text{g/mL}$ )	SD ( $\mu\text{g/mL}$ )	CV %
Bmix1-U	0.632	0.730	1221.57	140.75	11.52
	0.771				
	0.749				
	0.747				
	0.672				
0.811					

Table 3 – BCA Results of the undiluted pooled bovine sample (Bmix1-U).

Std# (pg/mL)	R&D				ENZO			
	RepliCts (A)	Mean (A)	SD (A)	CV %	RepliCts (A)	Mean (A)	SD (A)	CV %
2500	0.253	0.244	0.013	5.22	0.051	0.049	0.003	0.416
	0.235				0.047			
1250	0.345	0.336	0.012	3.57	0.083	0.082	0.001	0.847
	0.328				0.082			
625	0.438	0.425	0.018	4.33	0.143	0.140	0.005	0.648
	0.412				0.136			
313	0.512	0.492	0.028	5.75	0.227	0.226	0.001	0.312
	0.472				0.226			
156	0.547	0.528	0.026	4.95	0.329	0.328	0.002	0.548
	0.510				0.326			
78	0.578	0.556	0.030	5.46	0.415	0.418	0.004	0.857
	0.535				0.420			
39	0.595	0.573	0.031	5.43	0.511	0.510	0.002	5.772
	0.551				0.508			

Table 4 – Results of the R&D and ENZO dilution standards (std#).



Sample ID	R&D					ENZO				
	RepliCts (A)	Mean (A)	Conc (pg/mL)	SD (pg/mL)	CV %	RepliCts (A)	Mean (A)	Conc (pg/mL)	SD (pg/mL)	CV %
Undiluted	0.572	0.563	61.105	36.891	60.37	0.528	0.5215	33.914	3.205	9.45
	0.554					0.515				
1:2	0.600	0.586	{}	{}	{}	0.555	0.589	13.884	12.011	86.51
	0.572					0.623				
1:4	0.543	0.567	51.043	{}	{}	0.552	0.597	12.050	15.087	125.2
	0.590					0.641				
1:8	0.550	0.532	159.333	87.570	54.96	0.574	0.577	17.104	0.940	5.49
	0.513					0.579				
1:16	0.543	0.527	174.529	77.248	44.26	0.564	0.569	19.137	1.953	10.20
	0.511					0.574				
1:32	0.532	0.527	174.529	24.120	13.82	0.564	0.566	19.972	0.793	3.97
	0.522					0.568				
1:64	0.571	0.562	65.469	39.221	59.91	0.602	0.586	14.638	5.735	39.18
	0.552					0.570				
IAP 1:8	0.585	0.539	135.210	107.309	79.36	0.593	0.585	14.934	3.214	0.215
	0.570					0.601				
	0.546					0.564				
	0.509					0.582				
	0.520					0.585				
	0.503					0.584				
	0.521					0.585				
IAP 1:16	0.517	0.512	212.385	46.990	22.12	0.585	0.575	17.505	3.802	21.72
	0.529					0.572				
	0.500					0.589				
	0.529					0.566				
	0.501					0.553				
	0.585					0.607				
IAP 1:32	0.566	0.537	140.081	101.249	72.28	0.595	0.591	13.019	1.879	14.43
	0.534					0.589				
	0.510					0.591				
	0.525					0.588				
	0.504					0.585				
	0.496					0.607				
1:8Spike	0.380	0.438	595.048	307.095	51.61	0.204	0.204	365.352	0.000	0.00
	0.496					0.204				
1:16Spike	0.377	0.437	605.8165	317.864	52.47	0.176	0.179	449.794	13.500	3.00
	0.504					0.181				
1:32Spike	0.366	0.436	631.584	374.436	59.29	0.179	0.181	440.39	10.484	2.38
	0.657					0.183				
B <sub>0</sub>	0.651	0.654	{}	{}	{}	0.591	0.588	14.259	1.244	8.72
	0.584					0.584				
BLANK						-0.009	-0.003	{}	{}	{}
						0.003				
NSB	0.887	0.877	{}	{}	{}	0.468	0.468	55.255	{}	{}
	0.867					0.468				
TA						1.011	0.993	{}	{}	{}
						0.974				

Table 5 – R&D and ENZO results of the pooled bovine NP sample.



Sample ID	R&D			ENZO		
	[PGE2] (pg/mL)	[TP] (µg/mL)	[PGE2] / [TP] (pg/µg)	[PGE2] (pg/mL)	[TP] (µg/mL)	[PGE2] / [TP] (pg/µg)
Bmix1-U	61.105	1221.57	0.050	33.914	1221.57	0.028

Table 6 – PGE2 concentrations of the R&D and ENZO from table 5, related to the total protein ([TP]) concentrations of the BCA from table 3.

Sample ID	RepliCts (A)	Mean (A)	Conc (µg/mL)	SD (µg/mL)	CV %
Cmix-U	0.362	0.403	565.438	46.513	8.22
	0.392				
	0.408				
	0.412				
	0.411				
1:2	0.256	0.262	304.754	13.91	4.56
	0.267				
1:4	0.177	0.172	147.248	12.246	8.32
	0.167				
1:8	0.147	0.138	87.859	22.988	26.16
	0.128				
1:16	0.116	0.108	37.638	19.165	50.92
	0.100				

Table 7 – BCA Results of the undiluted (Cmix-U) pooled homogenized canine NP sample with corresponding dilution results.

Std# (pg/mL)	R&D				ENZO				ENZO-HS			
	RepliCts (A)	Mean (A)	SD (A)	CV %	RepliCts (A)	Mean (A)	SD (A)	CV %	RepliCts (A)	Mean (A)	SD (A)	CV %
2500	0.277	0.253	0.033	13.11	0.040				**	**	**	**
	0.230				0.075				0.073	0.003	3.901	
1250	0.365	0.374	0.013	3.587	0.101				0.071	0.120	0.006	5.303
	0.384				0.124							
625	0.449	0.455	0.008	1.865	0.167				0.116	0.200	0.018	9.169
	0.461				0.214							
313	0.522	0.534	0.018	3.307	0.260				0.188	0.280	0.038	24.200
	0.547				0.328							
156	0.549	0.576	0.037	6.512	0.346				0.232	0.508	0.031	6.119
	0.602				0.487							
78	0.606	0.601	0.007	1.177	0.414				0.530	0.702	0.025	3.525
	0.596				0.684							
39	0.615	0.630	0.021	3.367	0.446				0.720	1.004	0.023	2.324
	0.645				0.987							
18									1.020	0.996	0.011	1.065
					1.003							
9									0.988			

Table 8 – Results of the canine R&D, ENZO and ENZO-HS dilution standards (std#). Calibration line of the ENZO was in mono because of a double applied amount of conjugate.



Sample ID	R&D					ENZO					ENZO-HS				
	RepliCts (A)	Mean (A)	Conc (pg/mL)	SD (pg/mL)	CV %	RepliCts (A)	Mean (A)	Conc (pg/mL)	SD (pg/mL)	CV %	RepliCts (A)	Mean (A)	Conc (pg/ml)	SD (pg/mL)	CV %
Undiluted	0.623	0.628	31.593	13.898	43.99	0.452	0.470	19.503	21.576	110.63	0.692	0.680	46.812	2.297	4.91
	0.633					0.488					0.668				
1:2	0.619	0.643	5.512	{}	{}	0.472	0.487	4.972	{}	{}	0.876	0.850	26.901	3.539	13.16
	0.608					0.456					0.796				
	0.644					0.494					0.866				
	0.678					0.474					0.864				
	0.662					0.502					0.820				
	0.637					0.526					0.881				
	0.653					*0.588*									
	0.610					0.481					1.035				
1:4	0.583	0.609	72.036	{}	{}	0.481	0.495	{}	{}	{}	1.008	1.033	8.819	4.432	50.26
	0.578					0.508					0.977				
	0.623					0.512					1.068				
	0.653					*0.594*					1.086				
	0.563					0.498					1.136				
	0.594					0.502					1.029				
1:8	0.644	0.616	57.310	{}	{}	0.489	0.496	{}	{}	{}	1.028	1.092	1.249	{}	{}
	0.630					0.497					1.094				
	0.648					0.494					1.128				
	*1.123*					*0.528*					1.132				
	0.586					0.503					1.252				
	0.622					0.512					1.197				
1:16	0.602	0.612	66.343	{}	{}	0.514	0.511	{}	{}	{}	1.124	1.185	{}	{}	{}
	0.591					0.494					1.166				
	0.612					0.522					1.180				
	0.658					0.520					1.190				
	0.488					0.229					1.164				
	0.537					0.288					1.170				
1:2Spike	0.518	0.512	383.897	142.413	37.10	0.296	0.258	320.887	102.615	31.98	0.184	0.167	324.679	10.182	3.14
	0.566					0.280					0.154				
1:4Spike	0.577	0.542	271.237	120.456	44.41	0.306	0.288	253.739	22.559	8.89	0.202	0.169	317.651	59.486	18.73
	0.594					0.312					0.194				
1:8Spike	0.193	0.585	133.659	33.509	25.07	0.044	0.310	214.445	7.457	3.48	0.390	0.198	254.758	9.738	3.82
	0.190					0.044					0.194				
2500AdS	0.330	0.192	3766.535	50.931	1.35	0.076	0.044	2479.854	30.309	1.22					
1250AdS	0.316					0.074					0.058				
625AdS	0.435	0.432	789.869	29.925	3.79	0.116	0.121	963.223	57.977	6.02	0.083	0.089	1641.10	1751.80	106.75
	0.428					0.126					0.096				
313AdS	0.524	0.548	248.579	118.913	47.84	0.184	0.183	568.033	9.486	1.67	0.147	0.142	419.920	32.391	7.71
	0.573					0.182					0.138				
156AdS	0.601	0.613	63.655	38.839	61.01	0.262	0.252	337.067	39.679	11.77	0.238	0.216	228.610	43.697	19.11
	0.625					0.240					0.194				
78AdS	0.653	0.676	{}	{}	{}	0.296	0.313	208.356	40.286	19.33	0.390	0.352	124.070	24.108	19.43
	0.700					0.330					0.314				
39AdS	0.679	0.712	{}	{}	{}	0.351	0.348	154.232	6.066	3.93	0.408	0.400	105.090	3.366	3.20
	0.745					0.345					0.394				
Undiluted TNF-α	0.226	0.233	2894.145	190.387	6.58	0.005	0.005	6561.795	0.000	0.00	0.003	0.003	{}	{}	{}
	0.241					0.005					0.003				
1:2 TNF-α	0.324	0.332	1573.270	106.47	6.77	0.008	0.010	545.300	525.528	9.63	0.008	0.010	{}	{}	{}
	0.339					0.012					0.011				
1:4 TNF-α	0.401	0.426	826.672	216.203	26.15	0.018	0.019	4281.860	165.188	3.86	0.014	0.014	{}	{}	{}
	0.450					0.020					0.014				
1:8 TNF-α	0.470	0.500	438.943	182.770	41.64	0.039	0.038	2763.170	110.434	3.97	0.033	0.032	{}	{}	{}
	0.529					0.036					0.032				
1:16 TNF-α	0.576	0.600	95.060	85.743	90.20	0.072	0.072	1629.697	29.396	1.80	0.056	0.059	{}	{}	{}
	0.624					0.074					0.062				
1:32 TNF-α	0.602	0.613	65.210	37.066	59.30	0.126	0.123	945.269	43.851	4.64	0.117	0.113	674.02	85.25	12.65
	0.625					0.120					0.109				
1:64 TNF-α	0.629	0.648	{}	{}	{}	0.194	0.185	559.174	59.066	10.56	0.200	0.191	268.38	25.905	9.65
	0.667					0.176					0.182				
B <sub>0</sub> AdS	0.710	0.729	{}	{}	{}	0.380	0.412	74.342	48.246	64.90	0.554	0.592	59.875	9.031	15.08
	0.748					0.444					0.631				
B <sub>0</sub>	0.676	0.680	{}	{}	{}	0.710	0.600	{}	{}	{}	1.374	1.334	{}	{}	{}
	0.683					0.490					1.292				
BLANK						0.000	0.000	8199.734	0.000	0.00	0.002	0.003	{}	{}	{}
						0.000					0.004				
NSB	0.002	0.003	16795.75	132.694	0.79						0.965	0.957	16.372	1.167	7.13
	0.003									0.948					
TA						0.854	0.889	{}	{}	{}	2.160	2.287	{}	{}	{}
						0.924					2.414				
Bmix2-U	0.588	0.605	81.392	60.111	73.85	0.440	0.441	45.765	0.672	1.49	0.720	0.705	43.452	2.815	6.48
	0.623					0.442					0.690				
Undiluted °C -PGE2	0.587	0.611	67.116	79.749	118.82	0.440	0.440	47.194	1.35	2.86	1.670	1.630	{}	{}	{}
	0.636					0.438					1.590				
1:32°C -PGE2	0.597	0.600	93.795	12.501	13.33	0.250	0.300	232.542	132.1	56.80	0.240	0.248	190.701	12.253	6.43
	0.604					0.349					0.258				

Table 9 – R&D, ENZO and ENZO-HS ELISA results of the pooled homogenized canine NP sample and Bmix2-U.





Sample ID	R&D				ENZO				ENZO-HS			
	[PGE2] (pg/mL)	[TP] (µg/mL)	[PGE2]/[TP] (pg/µg)	[PGE2]/[TP] (%)	[PGE2] (pg/mL)	[TP] (µg/mL)	[PGE2]/[TP] (pg/µg)	[PGE2]/[TP] (%)	[PGE2] (pg/mL)	[TP] (µg/mL)	[PGE2]/[TP] (pg/µg)	[PGE2]/[TP] (%)
CanineNP Undiluted	31.593	565.438	0.056	5.59	19.503	565.438	0.035	3.45	46.812	565.438	0.083	8.28
CanineNP 1:2	5.512	304.754	0.018	1.81	4.972	304.754	0.016	1.63	26.901	304.754	0.088	8.83
CanineNP 1:4	72.036	147.248	0.489	48.92	( )	147.248	( )	( )	8.819	147.248	0.062	6.23
CanineNP 1:8	57.310	87.859	0.652	65.22	( )	87.859	( )	( )	1.249	87.859	0.100	10.04
CanineNP 1:16	66.343	37.638	1.763	176.27	( )	37.638	( )	( )	( )	37.638	( )	( )
Bmix-2U	81.392	1221.57	0.067	6.66	45.765	1221.57	0.037	3.75	43.452	1221.57	0.035	3.53

Table 10 – PGE2 concentrations of the R&D, ENZO and ENZO-HS from table 9, related to the total protein ([TP]) concentrations of the BCA from table 3 and table 7.

Std# (pg/mL)	RepliCts (A)	Mean (A)	SD (A)	CV %
1000	0.084	0.084	0.000	0.000
	0.084			
500	0.136	0.136	0.000	0.000
	0.136			
250	0.246	0.242	0.005	2.045
	0.238			
125	0.340	0.376	0.050	13.352
	0.412			
62	0.562	0.544	0.024	4.415
	0.528			
31	0.782	0.786	0.005	0.630
	0.790			
15	0.916	0.944	0.041	4.342
	0.973			
8	1.023	1.020	0.004	0.416
	1.017			

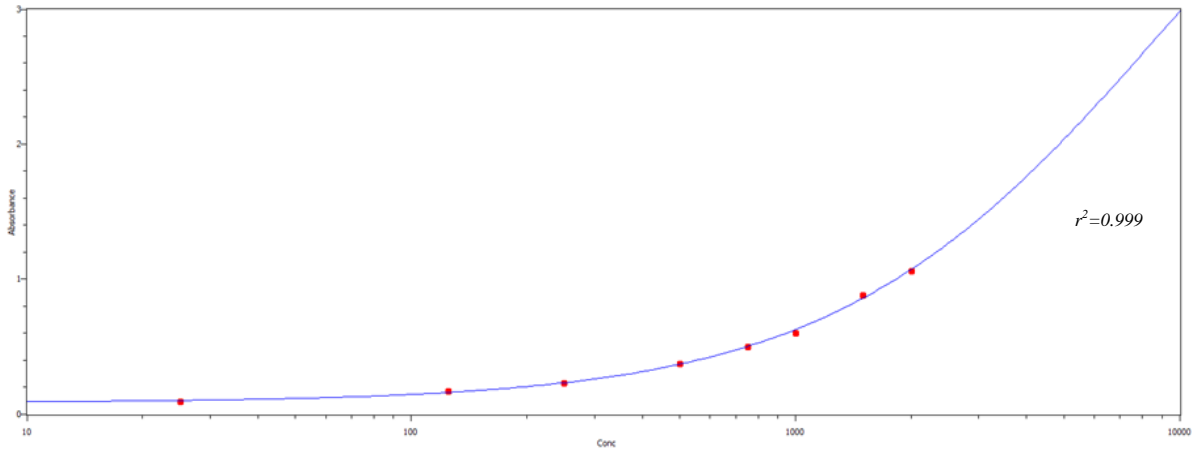
Table 11 – Results of the second ENZO-HS dilution standards (std#).

Sample ID	RepliCts (A)	Mean (A)	Conc (pg/mL)	SD (pg/mL)	CV %
Canine 5coupes	0.810	0.835	24.154	3.452	14.29
	0.860				
Canine 9coupes	0.542	0.546	66.933	1.271	1.90
	0.550				
Canine 10coupes	0.520	0.530	70.875	3.386	4.78
	0.540				
Canine 15coupes	0.426	0.430	100.146	2.070	2.07
	0.434				
1:8Bmix2	1.108	1.157	( )	( )	( )
	1.206				
1:16Bmix2	1.108	1.214	( )	( )	( )
	1.320				
1:32Bmix2	1.166	1.185	( )	( )	( )
	1.204				
Bo	1.231	1.217	( )	( )	( )
	1.202				
BLANK	0.001	0.001	( )	( )	( )
	0.001				
TA	2.154	2.173	( )	( )	( )
	2.192				

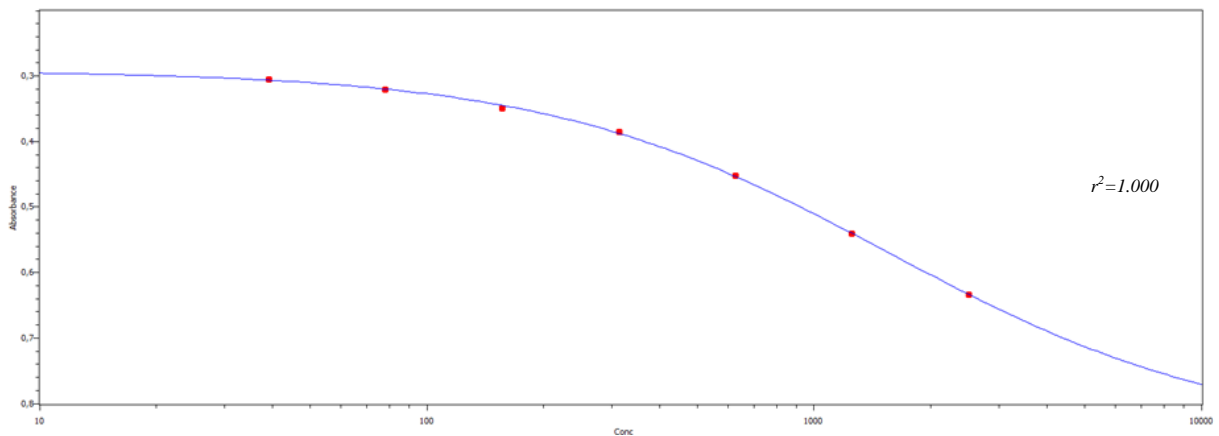
Table 12 – ENZO-HS sample results of the canine NP samples derived from 5, 9, 10 and 15 cryoslides, and the dilution results of the Bmix-2.



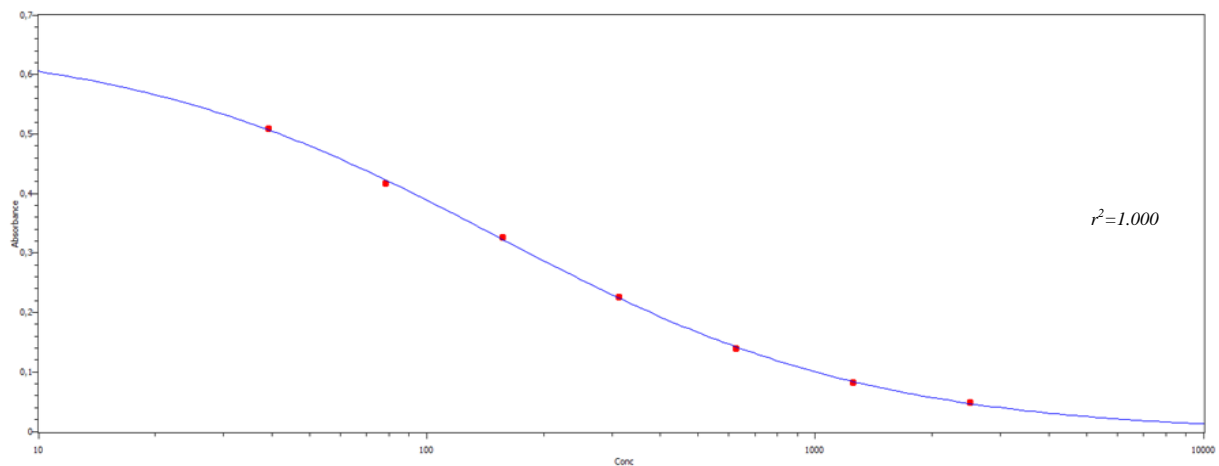
**Appendix B: list of result figures**



**Figure 8** – The BCA standard curve based on the absorbance rates (Vertical axis) from table 2. Concentrations are given in µg/mL.(Horizontal axis).



**Figure 9** – The R&D standard curve based on the absorbance rates (Vertical axis) from table 4. Concentrations are given in pg/mL.(Horizontal axis).



**Figure 10** – The ENZO standard curve based on the absorbance rates (Vertical axis) from table 4. Concentrations are given in pg/mL.(Horizontal axis).

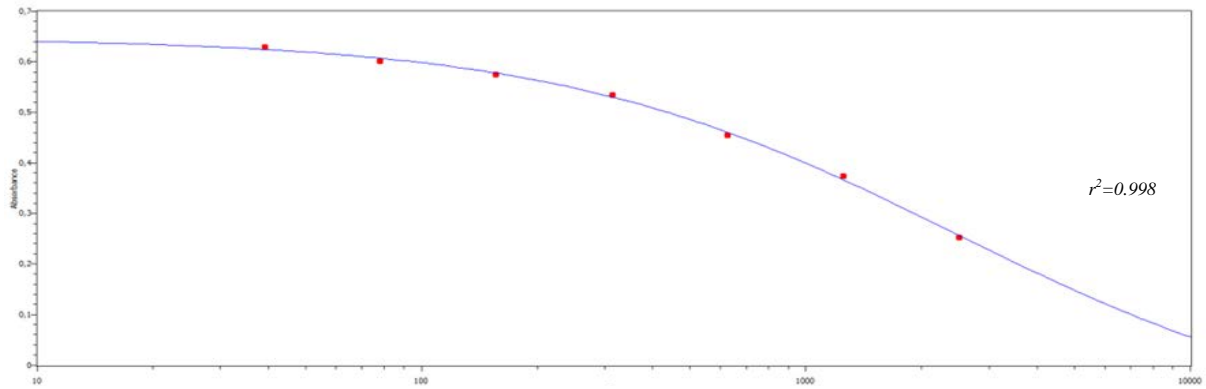


Figure 11 – The R&D standard curve based on the absorbance rates (Vertical axis) ,from table 8. Concentrations are given in pg/mL.(Horizontal axis).

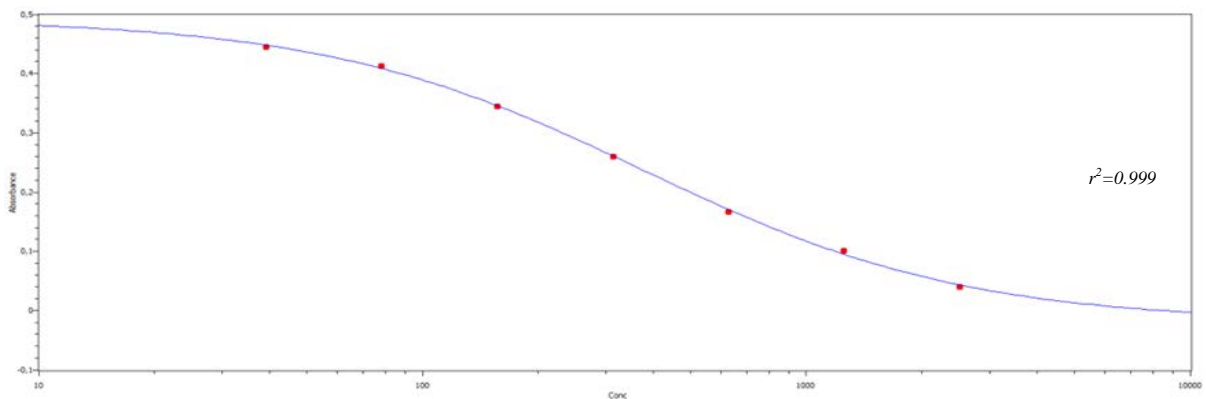


Figure 12 – The ENZO standard curve based on the absorbance rates (Vertical axis) ,from table 8. Concentrations are given in pg/mL.(Horizontal axis).

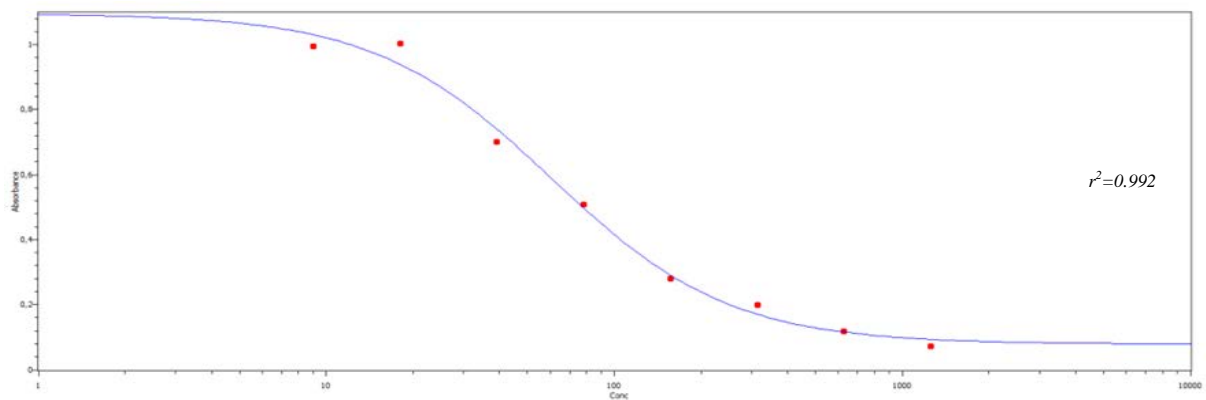
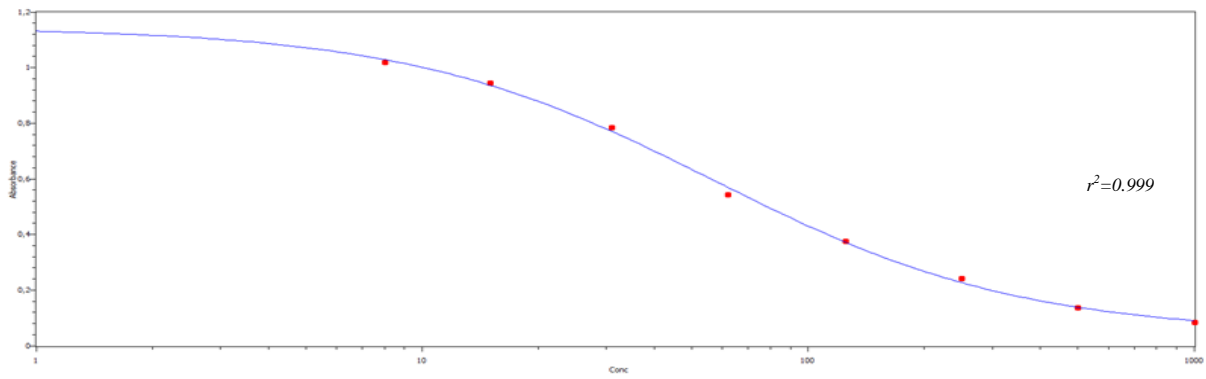


Figure 13 – The ENZO-HS standard curve based on the absorbance rates (Vertical axis) ,from table 8. Concentrations are given in pg/mL.(Horizontal axis).



**Figure 14**– The ENZO-HS standard curve based on the absorbance rates (Vertical axis) ,from table 11. Concentrations are given in pg/mL.(Horizontal axis).